The divine clockwork: Bohr's correspondence principle and Nelson's stochastic mechanics for the atomic elliptic state

JOURNAL OF MATHEMATICAL PHYSICS **49**, 032102 (2008)

The divine clockwork: Bohr's correspondence principle and Nelson's stochastic mechanics for the atomic elliptic state

Richard Durran, Andrew Neate,[a] and Aubrey Truman[b]
Department of Mathematics, Swansea University, Singleton Park, Swansea, SA2 8PP, Wales, United Kingdom

(Received 2 November 2007; accepted 4 January 2008; published online 6 March 2008)

We consider the Bohr correspondence limit of the Schrödinger wave function for an atomic elliptic state. We analyze this limit in the context of Nelson's stochastic mechanics, exposing an underlying deterministic dynamical system in which trajectories converge to Keplerian motion on an ellipse. This solves the long standing problem of obtaining Kepler's laws of planetary motion in a quantum mechanical setting. In this quantum mechanical setting, local mild instabilities occur in the Keplerian orbit for eccentricities greater than $\frac{1}{\sqrt{2}}$ which do not occur classically.
 [DOI: 10.1063/1.2837434]

I. BACKGROUND

A. Introduction

One of the longest standing problems in quantum mechanics is to obtain Kepler's laws of planetary motion by taking the Bohr correspondence limit of a suitable Schrödinger wave function for an atomic elliptic state. The Bohr correspondence limit of a quantum state is found by allowing the quantum numbers to become infinite while $\hbar$ becomes vanishingly small with the energies and angular momenta of the system fixed with physical values of order 1.[4] We have approached this quantum mechanical problem from the perspective of Nelson's stochastic mechanics.

In 1966, Nelson produced a new formulation of nonrelativistic quantum mechanics in terms of diffusion processes satisfying the Nelson–Newton law, a stochastic version of Newton's second law of motion.[12–14] This work was based on the assumption that every particle of mass m moves in a random environment driven by a Brownian motion with diffusion constant $\hbar/2m$. Some mathematical physicists felt that Nelson's formulation merely recapitulated the standard results of Schrödinger quantum mechanics without explaining the physical agency responsible for the Brownian noise in the system, and so the theory did not prove popular. However, the theory does give a new mental picture of the quantum world in which one can calculate the statistics of new observables, like first hitting times, which should be open to measurement.[8] Moreover, within this formulation, Nelson showed that the Nelson–Newton law leads uniquely to Schrödinger quantum mechanics, advocating the view that the Schrödinger equation is a way of linearizing a very complicated nonlinear system of equations equivalent to the Nelson–Newton law.

In this paper, we will use Nelson's stochastic mechanics to take the correspondence limit of the atomic elliptic state for the Coulomb potential and show that this limit gives Kepler's laws of planetary motion.

[a]Electronic mail: a.d.neate@swansea.ac.uk.
[b]Electronic mail: a.truman@swansea.ac.uk.

B. Nelson's stochastic mechanics

We begin with a brief account of Nelson's stochastic mechanics based on the summaries in Refs. 6 and 7. Let $\boldsymbol{X}$ be the position of a particle of unit mass diffusing in $\mathbb{R}^d$ according to an Itô stochastic differential equation with diffusion constant $\epsilon^2/2$,

$$\mathrm{d}\boldsymbol{X}(t) = \boldsymbol{b}(\boldsymbol{X}(t),t)\mathrm{d}t + \epsilon \mathrm{d}\boldsymbol{B}(t), \quad t > 0, \quad \boldsymbol{X}(0) = \boldsymbol{x}, \tag{1}$$

where $\boldsymbol{B}=(B_1,B_2,\ldots,B_d)$ is a d-dimensional Brownian motion process on a probability space $(\Omega,\mathcal{A}_t,\mathbb{P})$, with covariance

$$\mathbb{E}\{B_i(t)B_j(s)\} = \delta_{ij}(t \wedge s),$$

where $\mathbb{E}$ denotes the expectation with respect to the measure $\mathbb{P}$.

We assume that the process $\boldsymbol{X}$ has a smooth density function $\rho(\boldsymbol{y},t)$ such that for any $A \in \mathcal{A}_t$,

$$\mathbb{P}\{\boldsymbol{X}(t) \in A\} = \int_{\boldsymbol{y}\in A} \rho(\boldsymbol{y},t)\mathrm{d}\boldsymbol{y}.$$

Then, the density ρ must satisfy the forward Kolmogorov equation

$$\frac{\partial \rho}{\partial t}(\boldsymbol{y},t) = \nabla \cdot \left(\frac{\epsilon^2}{2} \nabla \rho(\boldsymbol{y},t) - \rho(\boldsymbol{y},t)\boldsymbol{b}(\boldsymbol{y},t) \right). \tag{2}$$

We define the mean forward and backward derivatives $D_\pm$ by

$$D_\pm f(\boldsymbol{X}(t),t) := \lim_{h\downarrow 0} \mathbb{E}\left\{ \frac{f(\boldsymbol{X}(t\pm h),t\pm h) - f(\boldsymbol{X}(t),t)}{\pm h} \middle| \boldsymbol{X}(t) \right\}.$$

Assuming some mild regularity conditions on f, Itô's formula gives

$$D_+ f(\boldsymbol{X}(t),t) = \left(\frac{\partial}{\partial t} + \boldsymbol{b}(\boldsymbol{X}(t),t)\cdot\nabla + \frac{\epsilon^2}{2}\Delta \right) f(\boldsymbol{X}(t),t).$$

In particular, it follows that the mean forward velocity is simply

$$\boldsymbol{b}_+(\boldsymbol{X}(t),t) := D_+\boldsymbol{X}(t) = \boldsymbol{b}(\boldsymbol{X}(t),t).$$

Furthermore, it can be shown that for $g=g(\boldsymbol{X}(t),t)$ and $h=h(\boldsymbol{X}(t),t)$,

$$\frac{\mathrm{d}}{\mathrm{d}t}\mathbb{E}\{gh\} = \mathbb{E}\{gD_-h\} + \mathbb{E}\{hD_+g\},$$

and it follows, using integration by parts, that for $f=f(\boldsymbol{X}(t),t)$,

$$D_- f = \left(\frac{\partial}{\partial t} + (\boldsymbol{b}_+ - \epsilon^2 \nabla \ln \rho)\cdot\nabla - \frac{\epsilon^2}{2}\Delta \right) f.$$

This gives the mean backward velocity as

$$\boldsymbol{b}_-(\boldsymbol{X}(t),t) := D_-\boldsymbol{X}(t) = \boldsymbol{b}_+(\boldsymbol{X}(t),t) - \epsilon^2 \nabla \ln \rho(\boldsymbol{X}(t),t).$$

We can also introduce the osmotic velocity $\boldsymbol{u}$ and the current velocity $\boldsymbol{v}$ such that

$$\boldsymbol{u} := \tfrac{1}{2}(\boldsymbol{b}_+ - \boldsymbol{b}_-), \quad \boldsymbol{v} := \tfrac{1}{2}(\boldsymbol{b}_+ + \boldsymbol{b}_-). \tag{3}$$

If we now define the stochastic acceleration by

$$\boldsymbol{a}(\boldsymbol{X}(t),t) = \tfrac{1}{2}(D_+D_- + D_-D_+)\boldsymbol{X}(t),$$

then it follows that

$$\boldsymbol{a}(\boldsymbol{X}(t),t) = \left(\frac{\partial \boldsymbol{v}}{\partial t} + (\boldsymbol{v}\cdot\nabla)\boldsymbol{v} - (\boldsymbol{u}\cdot\nabla)\boldsymbol{u} - \frac{\epsilon^2}{2}\Delta\boldsymbol{u}\right)(\boldsymbol{X}(t),t). \tag{4}$$

We now show how this apparently impenetrable expression takes on a deep significance in connection with the Schrödinger equation.

Consider a quantum mechanical particle of unit mass in $\mathbb{R}^d$ subject to the force field $-\nabla V$, where V is some real valued potential. The corresponding complex valued wave function ψ satisfies the Schrödinger equation

$$i\hbar\frac{\partial\psi}{\partial t} = -\frac{\hbar^2}{2}\Delta\psi + V\psi, \tag{5}$$

where (letting ψ^* denote the complex conjugate of ψ) the quantum mechanical particle density is

$$\rho = |\psi|^2 = \psi\psi^*.$$

Multiplying through Eq. (5) by ψ^* gives the equivalent Schrödinger equation

$$i\hbar\psi^*\frac{\partial\psi}{\partial t} = -\frac{\hbar^2}{2}\psi^*\Delta\psi + V|\psi|^2. \tag{6}$$

Equating imaginary parts in (6) gives the continuity equation

$$\frac{\partial\rho}{\partial t} + \nabla\cdot j = 0, \tag{7}$$

where j is the probability current,

$$j = \frac{\hbar}{2i}(\psi^*\nabla\psi - \psi\nabla\psi^*).$$

If we now write

$$\psi = \exp(R + iS),$$

where R and S are real valued functions of space and time, then it follows that

$$\rho = \exp(2R), \quad j = \hbar\rho\nabla S.$$

The continuity equation (7) now becomes

$$\frac{\partial\rho}{\partial t} = \nabla\cdot(-\hbar\nabla S e^{2R}) = \nabla\cdot\left(\frac{\hbar}{2}\nabla e^{2R} - \hbar e^{2R}\nabla(R+S)\right).$$

Therefore, if we let

$$\epsilon^2 = \hbar, \quad \boldsymbol{b} = \hbar\nabla(R+S),$$

then we have

$$\frac{\partial\rho}{\partial t} = \nabla\cdot\left(\frac{\epsilon^2}{2}\nabla\rho - \rho\boldsymbol{b}\right).$$

This is the forward Kolmogorov equation (2) for a diffusion $\boldsymbol{X}(t)$ with forward and backward velocities,

$$\boldsymbol{b}_+(\boldsymbol{X}(t),t) = \epsilon^2 \nabla (R+S), \quad \boldsymbol{b}_-(\boldsymbol{X}(t),t) = \epsilon^2 \nabla (S-R). \tag{8}$$

A tedious calculation from Eqs. (3), (4), and (8) gives the stochastic acceleration in terms of R and S as

$$\boldsymbol{a}(\boldsymbol{X}(t),t) = -\nabla\left(-\epsilon^2\frac{\partial S}{\partial t} + \frac{\epsilon^4}{2}(|\nabla R|^2 - |\nabla S|^2 + \Delta R)\right)(\boldsymbol{X}(t),t). \tag{9}$$

However, equating real parts of Eq. (6) gives

$$\frac{\partial S}{\partial t} = \frac{\epsilon^2}{2}(|\nabla R|^2 - |\nabla S|^2 + \Delta R) - \frac{V}{\epsilon^2}. \tag{10}$$

Therefore, combining Eqs. (9) and (10) gives

$$\boldsymbol{a}(\boldsymbol{X}(t),t) = -\nabla V(\boldsymbol{X}(t),t), \tag{11}$$

where V is the potential in the Schrödinger equation. Equation (11) is the Nelson–Newton law for a particle of unit mass.

The Nelson–Newton law argues that to investigate the Bohr correspondence limit of a quantum state, we should investigate the Nelson diffusion process in the appropriate limit.

C. Outline of the paper

Section II starts from Pauli's elegant solution of the hydrogen atom. We follow the results of Lena *et al.*[11] to obtain the Schrödinger wave function corresponding to an atomic elliptic state in $\mathbb{R}^3$ and then find its related Nelson diffusion process. In Sec. III, we derive the formal limiting wave function for this atomic elliptic state according to Bohr's prescription. We derive the corresponding limiting Nelson diffusion and present simulations of the limiting process showing how the process converges in large times to a particular ellipse, which we call the Kepler ellipse. We investigate the behavior of the drift for this limiting diffusion and demonstrate that it has a finite jump discontinuity across part of the semimajor axis of the Kepler ellipse. This singularity is the Bohr correspondence limit of the nodal surfaces of the atomic elliptic state wave function.

For the remainder of the paper, we restrict our wave functions and diffusion processes to the putative plane of motion ($z=0$). In Sec. IV, we introduce a new set of elliptic coordinates, the nonorthogonal Keplerian elliptic coordinates, and show how these greatly simplify the limiting Nelson diffusion process.

In Sec. V, we analyze the two dimensional limiting diffusion process. We discuss the behavior of the invariant measure for this system and demonstrate that it is sharply peaked on the Kepler ellipse. Taking an idea from the earlier work on excursions in stochastic mechanics,[19] we introduce a similarity transform for the generator of the Nelson diffusion process and use this to discuss the convergence over time of the density for the Nelson diffusion processes to their invariant measures. We also show that there is a positive probability of hitting the drift singularity in a finite time. Thus, to avoid inventing an artificial boundary condition, we restrict our path space so that our diffusing particle avoids this singularity and we estimate the probability for this to happen. On the restricted path space, we see that the Bohr correspondence limit reduces to the underlying deterministic dynamical system.

In Sec. VI, we look in detail at this underlying deterministic dynamical system. We show that this system has the Kepler ellipse as a stable periodic orbit and we derive Kepler's laws of planetary motion for a particle on this orbit. We identify which paths avoid the singularity and for these paths discuss the asymptotic stability of the Kepler ellipse. We show that the invariant density can be used to construct a Lyapunov function for the system. Using this, we show that all motions starting outside the Kepler ellipse converge to the Keplerian motion on the Kepler ellipse. For motions starting inside the Kepler ellipse, the result is more difficult to prove and we leave this to a future publication. We conclude by highlighting some surprising symmetries within the diffusion process and use these symmetries to show that mild local instabilities occur in the

dynamical system for $e > \frac{1}{\sqrt{2}}$ where e is the eccentricity of the Kepler ellipse.

Thus, we see that in $\mathbb{R}^2$, for orbits starting outside the Kepler ellipse and avoiding the singularity, the long time behavior of the Bohr correspondence limit of Nelson's stochastic mechanics for atomic elliptic states is the Keplerian motion on the Kepler ellipse. We believe that we can extend this result to $\mathbb{R}^3$ but so far we have not found a convenient coordinate system in which to carry out the analysis.

II. THE ATOMIC ELLIPTIC STATE

A. The wave function for the atomic elliptic state

In this section, we follow the work of Lena *et al.*[11] Recall that the atomic circular state $|\text{Circ}\rangle_n$ corresponding to a Keplerian circular orbit is given by

$$\langle \boldsymbol{x}|\text{Circ}\rangle_n = \Psi_{n,n-1,n-1}(\boldsymbol{x}),$$

where $\boldsymbol{x}=(x,y,z)$ and $\Psi_{n,l,m}$ (with $l=0,1,\ldots,n-1, |m|\leqslant l$ and $m,n\in\mathbb{N}$) is the nodal Schrödinger wave function for the Hamiltonian

$$H(\boldsymbol{p},\boldsymbol{q}) = \frac{\boldsymbol{p}^2}{2} - \frac{\mu}{|\boldsymbol{q}|}. \tag{12}$$

The vectors $\boldsymbol{p}=(p_1,p_2,p_3)$ and $\boldsymbol{q}=(q_1,q_2,q_3)$ are the momentum and position operators in Cartesian coordinates for the orbiting quantum particle with $[q_k,p_l]=i\hbar\delta_{kl}$ for $k,l=1,2,3$. We now work in suitable units so that $\hbar=1$ and $\mu=1$. Then, for the orbital angular momentum $\boldsymbol{L}$, where

$$\boldsymbol{L} = (L_1,L_2,L_3) = (\boldsymbol{q}\times\boldsymbol{p}), \quad \boldsymbol{L}^2 = (L_1^2+L_2^2+L_3^2),$$

we have

$$\boldsymbol{L}^2\Psi_{n,l,m} = l(l+1)\Psi_{n,l,m}, \quad L_3\Psi_{n,l,m} = m\Psi_{n,l,m}, \quad H\Psi_{n,l,m} = -\frac{1}{2n^2}\Psi_{n,l,m}.$$

The state we consider is

$$|\text{Elliptic}(\theta)\rangle_n = \exp(-i\theta A_2)|\text{Circ}\rangle_n, \tag{13}$$

where

$$\boldsymbol{A} = (A_1,A_2,A_3) = \frac{1}{\sqrt{-2E}}\left(\frac{(\boldsymbol{p}\times\boldsymbol{L}-\boldsymbol{L}\times\boldsymbol{p})}{2} - \frac{\boldsymbol{q}}{|\boldsymbol{q}|}\right)$$

is the Hamilton–Lenz–Runge vector on the eigenspace of H with eigenvalue E. We will show that on the space where $E=E_n=-1/(2n^2)$, the state $|\text{Elliptic}(\theta)\rangle_n$ as $n\uparrow\infty$ corresponds to the elliptic atomic state with eccentricity $e=\sin\theta$ for some $\theta\in(0,\pi)$.

Pauli proved the fundamental identities

$$[A_1,A_2] = iL_3, \quad [A_2,L_3] = iA_1, \quad [L_3,A_1] = iA_2,$$

showing that A_1,A_2,L_3 (the constants of motion in the two dimensional problem) generate the dynamical symmetry group SO(3) for this situation. Now, define

$$\langle L_3\rangle(\theta) = \langle \text{Elliptic}(\theta)|L_3|\text{Elliptic}(\theta)\rangle,$$

$$\langle A_1\rangle(\theta) = \langle \text{Elliptic}(\theta)|A_1|\text{Elliptic}(\theta)\rangle.$$

It follows that

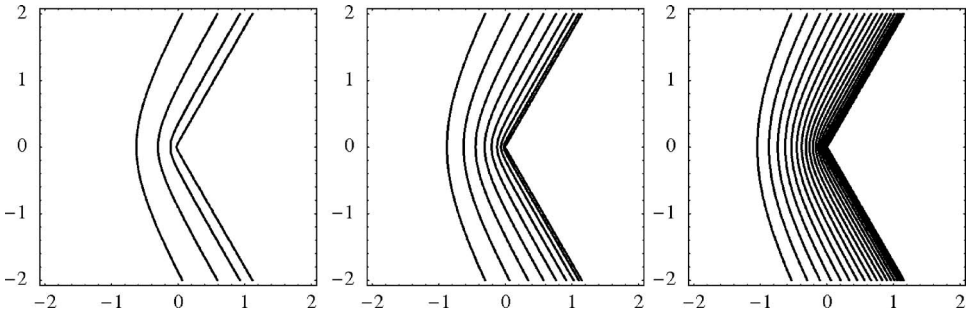

FIG. 1. The nodal surfaces in the (x,z) plane for $\psi_{\epsilon,n}$ for $e=0.5$ and $n=5$, 10, 20.

$$\frac{\mathrm{d}^2}{\mathrm{d}\theta^2}\langle L_3\rangle(\theta) = -\langle L_3\rangle(\theta), \quad \frac{\mathrm{d}^2}{\mathrm{d}\theta^2}\langle A_1\rangle(\theta) = -\langle A_1\rangle(\theta),$$

giving

$$\langle L_3\rangle(\theta) = (n-1)\cos(\theta), \quad \langle A_1\rangle(\theta) = (n-1)\sin(\theta).$$

Moreover, if we consider the classical identity relating the eccentricity e of the elliptic orbit to the angular momentum $\boldsymbol{L}$ and the energy E,

$$e^2 = 1 + 2\boldsymbol{L}^2 E,$$

and take the limit as $n\to\infty$, we find $e^2=\sin^2(\theta)$ as asserted. A clever argument using coherent state representations and the Kustaanheimo–Stiefel transformation yields, for $\theta_0=\arcsin(e)$, where $0<e<1$, to within a multiplicative constant (after reinstating $\hbar$ and the force constant μ),

$$\psi_{\epsilon,n}(\boldsymbol{x}) := \langle x|\mathrm{Elliptic}(\theta_0)\rangle_n = \exp\left(-\frac{n\mu}{\lambda^2}|\boldsymbol{x}|\right)\mathcal{L}_{n-1}(n\nu), \tag{14}$$

where

$$\nu = \frac{\mu}{\lambda^2}\left(|\boldsymbol{x}| - \frac{x}{e} - \frac{iy\sqrt{1-e^2}}{e}\right), \tag{15}$$

with $\boldsymbol{x}=(x,y,z)$, $E_n=-\mu^2/(2\lambda^2)$, $\epsilon^2=\hbar$, $\lambda=n\epsilon^2$, and $\mathcal{L}_{n-1}$ a Laguerre polynomial.

The nodes of the wave function $\psi_{\epsilon,n}$ are located on a series of $(n-1)$ hyperbolas in the plane $y=0$ each with axis x, eccentricity $1/e$ and focus at the origin (see Fig. 1).

Associated with the atomic elliptic state $|\mathrm{Elliptic}(\theta_0)\rangle_n$ where $\arcsin\theta_0=e$, there is a special ellipse which we will call the Kepler ellipse.

Definition 1: The Kepler ellipse is the ellipse in the plane $z=0$ with eccentricity e and semi-major axis a with one focus at the origin given in cylindrical polar coordinates by

$$\tilde{r} = \frac{a(1-e^2)}{1+e\cos\theta}, \quad z=0, \tag{16}$$

where $a=\lambda^2/\mu$, $x=\tilde{r}\cos\theta$, and $y=\tilde{r}\sin\theta$ with $\tilde{r}=\sqrt{x^2+y^2}$.

We will show that the correspondence limit of the Nelson diffusion for the atomic elliptic state with wave function $\psi_{\epsilon,n}$ is the Keplerian motion on the Kepler ellipse.

Remark 1: Throughout this work, e will refer to the eccentricity associated with the atomic elliptic state. When we use the exponential function, we shall always write $\exp(x)$ rather than e^x to avoid confusion.

B. The Nelson diffusion for the atomic elliptic state

We now derive the Nelson diffusion process $\boldsymbol{X}^{\epsilon,n}$ associated with the wave function $\psi_{\epsilon,n}$ for the atomic elliptic state $|\text{Elliptic}(\theta_0)\rangle_n$. If we write $\psi_{\epsilon,n}=\exp(R_{\epsilon,n}+iS_{\epsilon,n})$, then $\boldsymbol{X}^{\epsilon,n}$ satisfies

$$\mathrm{d}\boldsymbol{X}^{\epsilon,n}(t)=\boldsymbol{b}_{\epsilon,n}(\boldsymbol{X}^{\epsilon,n}(t))\mathrm{d}t+\epsilon\mathrm{d}\boldsymbol{B}(t),$$

with

$$\boldsymbol{b}_{\epsilon,n}=\epsilon^2\nabla(R_{\epsilon,n}+S_{\epsilon,n}).$$

We will now find the drift $\boldsymbol{b}_{\epsilon,n}$ for the atomic elliptic state.

The wave function $\psi_{\epsilon,n}(\boldsymbol{x})$ satisfies the Schrödinger equation

$$-\frac{1}{2}\epsilon^4\Delta\psi_{\epsilon,n}(\boldsymbol{x})-\frac{\mu}{|\boldsymbol{x}|}\psi_{\epsilon,n}(\boldsymbol{x})=E_n\psi_{\epsilon,n}(\boldsymbol{x}),$$

where $\epsilon^2=\hbar$, $E_n=-\mu^2/(2\lambda^2)$, $\lambda=n\epsilon^2$, and $\boldsymbol{x}=(x,y,z)$. Defining $\boldsymbol{Z}_{\epsilon,n}(\boldsymbol{x})$ by

$$\boldsymbol{Z}_{\epsilon,n}(\boldsymbol{x}):=-i\epsilon^2\frac{\nabla\psi_{\epsilon,n}(\boldsymbol{x})}{\psi_{\epsilon,n}(\boldsymbol{x})}=\epsilon^2\nabla(S_{\epsilon,n}-iR_{\epsilon,n}),\tag{17}$$

it follows that

$$-\frac{i\epsilon^2}{2}\nabla\cdot\boldsymbol{Z}_{\epsilon,n}(\boldsymbol{x})+\frac{1}{2}\boldsymbol{Z}_{\epsilon,n}^2(\boldsymbol{x})-\frac{\mu}{|\boldsymbol{x}|}=E_n,\tag{18}$$

where in Cartesians $\boldsymbol{Z}_{\epsilon,n}$ can be written as

$$\boldsymbol{Z}_{\epsilon,n}(\boldsymbol{x})=\frac{i\mu}{\lambda}\left(1-\frac{\mathcal{L}'_{n-1}(n\nu)}{\mathcal{L}_{n-1}(n\nu)}\right)\frac{\boldsymbol{x}}{|\boldsymbol{x}|}+\frac{\mu}{\lambda e}\frac{\mathcal{L}'_{n-1}(n\nu)}{\mathcal{L}_{n-1}(n\nu)}(i,-\sqrt{1-e^2},0),\tag{19}$$

and ν is defined in Eq. (15).

Combining Eqs. (17) and (19), the drift for the diffusion $\boldsymbol{X}^{\epsilon,n}$ is

$$\boldsymbol{b}_{\epsilon,n}(\boldsymbol{x})=\epsilon^2\nabla(R_{\epsilon,n}+S_{\epsilon,n})=\Re(\boldsymbol{Z}_{\epsilon,n}(\boldsymbol{x}))-\Im(\boldsymbol{Z}_{\epsilon,n}(\boldsymbol{x})),\tag{20}$$

where $\Re$ denotes the real part and $\Im$ denotes the imaginary part.

Clearly, from Eq. (19), the drift field $\boldsymbol{b}_{\epsilon,n}$ will have curves of singularities in the plane $y=0$ corresponding to the nodal curves of the wave function $\psi_{\epsilon,n}$ shown in Fig. 1 and also to the point $|\boldsymbol{x}|=0$. These singularities can be seen in Fig. 2 which shows the x component of the drift in the plane $z=0$. The line of singularities corresponds to the intersection of the nodal curves with the plane $z=0$. As discussed in Ref. 3, at each of these nodes, the drift is infinitely repulsive with the drift components becoming plus or minus infinity depending on the direction of approach. This means that the nodes will be effectively inaccessible to the diffusion process. As n increases, the number and density of the nodes will also increase.

The invariant measure for the wave function $\psi_{\epsilon,n}$ in the plane $z=0$ is shown in Fig. 3 together with simulations of $\boldsymbol{X}^{\epsilon,n}$. The invariant measure has a clear peak on an ellipse in the plane $z=0$. Away from this plane, it tends toward zero.

III. THE LIMITING ATOMIC ELLIPTIC STATE

A. The limiting wave function

We now derive the Bohr correspondence limit of the wave function $\psi_{\epsilon,n}$ as $n\to\infty$ and $\epsilon\to 0$ with $\lambda=\epsilon^2 n$ fixed. Recall the function $\boldsymbol{Z}_{\epsilon,n}$ from Eq. (17). We define the Bohr correspondence limit of $\boldsymbol{Z}_{\epsilon,n}$ as

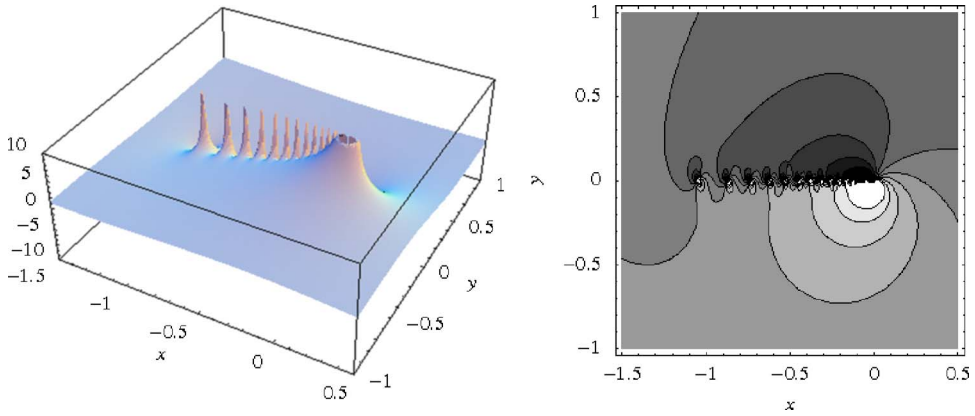

FIG. 2. (Color online) The x component of the drift $\boldsymbol{b}_{\epsilon,n}$ in the plane $z=0$ for $n=20$ and $e=0.5$ shown as a surface plot and a contour plot (black$=-\infty$; white$=+\infty$).

$$\boldsymbol{Z}_{0,\infty}(\boldsymbol{x}) := \lim_{\substack{n\uparrow\infty,\epsilon\downarrow 0 \\ \lambda=n\epsilon^2}} \boldsymbol{Z}_{\epsilon,n}(\boldsymbol{x}),$$

where the limit is taken with λ as a fixed real number.

In what follows, the Laguerre polynomials $\mathcal{L}_n(x)$ are defined according to the conventions in Ref. 5.

Lemma 1: Let $\mathcal{L}_n(x)$ denote the nth Laguerre polynomial and λ be a fixed real number. Then,

$$\lim_{\substack{n\uparrow\infty,\epsilon\downarrow 0 \\ \lambda=n\epsilon^2}} \frac{\mathcal{L}'_{n-1}(n\nu)}{\mathcal{L}_{n-1}(n\nu)} = \frac{1}{2}\left(1-\sqrt{1-\frac{4}{\nu}}\right).$$

Proof: For Laguerre polynomials,

$$v\mathcal{L}'_{n-1}(v) = (n-1)\mathcal{L}_{n-1}(v) - (n-1)\mathcal{L}_{n-2}(v),$$

and so

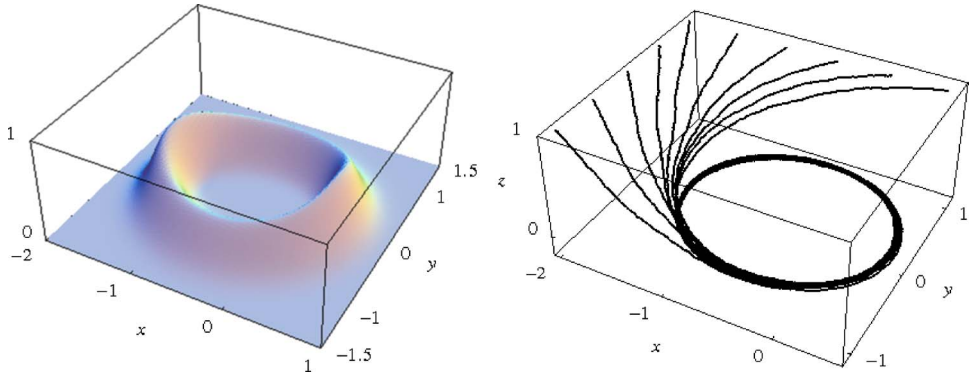

FIG. 3. (Color online) The invariant measure in the plane $z=0$ for the wave function $\psi_{\epsilon,n}$ and simulations of the process $\boldsymbol{X}^{\epsilon,n}$ for $n=20$ and $e=0.5$.

$$\frac{\mathcal{L}'_{n-1}(v)}{\mathcal{L}_{n-1}(v)} = \frac{n-1}{v} - \frac{n-1}{v}\frac{\mathcal{L}_{n-2}(v)}{\mathcal{L}_{n-1}(v)}.$$

Setting $v = n\nu$ gives

$$\lim_{\substack{n\uparrow\infty,\epsilon\downarrow 0\\ \lambda=n\epsilon^2}} \frac{\mathcal{L}'_{n-1}(n\nu)}{\mathcal{L}_{n-1}(n\nu)} = \frac{1}{\nu} - \frac{1}{\nu}\lim_{\substack{n\uparrow\infty,\epsilon\downarrow 0\\ \lambda=n\epsilon^2}} \frac{\mathcal{L}_{n-2}(n\nu)}{\mathcal{L}_{n-1}(n\nu)}.$$

However, Laguerre polynomials also satisfy the recurrence relation

$$n\mathcal{L}_n(v) - (2n-1-v)\mathcal{L}_{n-1}(v) + (n-1)\mathcal{L}_{n-2}(v) = 0.$$

Thus, if the limit,

$$p = \lim_{\substack{n\uparrow\infty,\epsilon\downarrow 0\\ \lambda=n\epsilon^2}} \frac{\mathcal{L}_{n-2}(n\nu)}{\mathcal{L}_{n-1}(n\nu)},$$

exists and is nonzero, then necessarily p satisfies

$$\frac{1}{p} - (2-\nu) + p = 0,$$

proving the lemma. □

Applying Lemma 1 to $\boldsymbol{Z}_{\epsilon,n}$ gives, in Cartesians,

$$\boldsymbol{Z}_{0,\infty}(\boldsymbol{x}) = \frac{i\mu}{2\lambda}\left(1 + \sqrt{1-\frac{4}{\nu}}\right)\frac{\boldsymbol{x}}{|\boldsymbol{x}|} + \frac{\mu}{2\lambda e}\left(1 - \sqrt{1-\frac{4}{\nu}}\right)(i, -\sqrt{1-e^2}, 0), \tag{21}$$

where, as expected from Eq. (18),

$$\frac{1}{2}\boldsymbol{Z}^2_{0,\infty}(\boldsymbol{x}) - \frac{\mu}{|\boldsymbol{x}|} = -\frac{\mu^2}{2\lambda^2}.$$

Proposition 1: The Bohr correspondence limit of the wave function $\psi_{\epsilon,n}$ for the atomic elliptic state gives the formal limiting wave function

$$\psi_\epsilon(\boldsymbol{x}) = \nu^{\lambda/\epsilon^2}\left(1 + \sqrt{1-\frac{4}{\nu}}\right)^{2\lambda/\epsilon^2} \exp\left(-\frac{\mu}{\lambda\epsilon^2}|\boldsymbol{x}| + \frac{\lambda\nu}{2\epsilon^2}\left(1 - \sqrt{1-\frac{4}{\nu}}\right)\right). \tag{22}$$

Proof: For the vector $\boldsymbol{Z}_{0,\infty}$, the function ψ_ϵ is the formal wave function satisfying

$$\boldsymbol{Z}_{0,\infty}(\boldsymbol{x}) = -i\epsilon^2\frac{\nabla\psi_\epsilon(\boldsymbol{x})}{\psi_\epsilon(\boldsymbol{x})}. \tag{23}$$

This wave function corresponds to Bohr's limit but is only an approximate solution of the Schrödinger equation. □

B. The limiting Nelson diffusion process

We now construct the limiting Nelson diffusion $\boldsymbol{X}^\epsilon$ corresponding to the limiting wave function ψ_ϵ. As in Eq. (17),

$$\boldsymbol{Z}_{0,\infty}(\boldsymbol{x}) = -i\epsilon^2 \frac{\nabla \psi_\epsilon(\boldsymbol{x})}{\psi_\epsilon(\boldsymbol{x})} = \epsilon^2 \nabla (S_\epsilon - iR_\epsilon),$$

where $\psi_\epsilon(\boldsymbol{x}) = \exp(R_\epsilon + iS_\epsilon)$. The subscripts emphasize the ϵ dependence in R_ϵ and S_ϵ arising from the ϵ^2.

Proposition 2: The limiting Nelson diffusion process $\boldsymbol{X}^\epsilon$ corresponding to the limiting wave function ψ_ϵ satisfies the Itô equation

$$\mathrm{d}\boldsymbol{X}^\epsilon(s) = \boldsymbol{b}(\boldsymbol{X}^\epsilon(s))\mathrm{d}s + \epsilon \mathrm{d}\boldsymbol{B}(s),$$

where $\boldsymbol{b}(\boldsymbol{x}) = (b_x, b_y, b_z)$ in Cartesian coordinates with

$$b_x = \frac{\mu}{2\lambda}\left\{(\alpha+\beta-1)\frac{1}{e} - (\alpha+\beta+1)\frac{x}{|\boldsymbol{x}|}\right\}, \tag{24a}$$

$$b_y = \frac{\mu}{2\lambda}\left\{(\alpha-\beta-1)\frac{\sqrt{1-e^2}}{e} - (\alpha+\beta+1)\frac{y}{|\boldsymbol{x}|}\right\}, \tag{24b}$$

$$b_z = -\frac{\mu}{2\lambda}(\alpha+\beta+1)\frac{z}{|\boldsymbol{x}|} \tag{24c}$$

and

$$\alpha = \left(\frac{1}{2}\sqrt{\frac{(e|\boldsymbol{x}| - x - 4\lambda^2 e/\mu)^2 + (1-e^2)y^2}{(e|\boldsymbol{x}|-x)^2 + (1-e^2)y^2}} + \frac{1}{2}\frac{(e|\boldsymbol{x}| - x - 2\lambda^2 e/\mu)^2 + (1-e^2)y^2 - 4\lambda^4 e^2/\mu^2}{(e|\boldsymbol{x}|-x)^2 + (1-e^2)y^2}\right)^{1/2}, \tag{25a}$$

$$\beta = \frac{-2\lambda^2 e\sqrt{1-e^2}\,y}{\mu((e|\boldsymbol{x}|-x)^2 + (1-e^2)y^2)\alpha}. \tag{25b}$$

Proof: The drift term in the limiting Nelson diffusion process $\boldsymbol{X}^\epsilon$ corresponding to the limiting wave function ψ_ϵ is

$$\boldsymbol{b}(\boldsymbol{x}) = \epsilon^2 \nabla (R_\epsilon + S_\epsilon) = \Re(\boldsymbol{Z}_{0,\infty}(\boldsymbol{x})) - \Im(\boldsymbol{Z}_{0,\infty}(\boldsymbol{x})).$$

A simple calculation gives [for ν as in Eq. (15)]

$$\sqrt{1 - \frac{4}{\nu}} = \alpha + i\beta,$$

and the result follows. □

Moreover, we can also find the functions R_ϵ and S_ϵ explicitly,

$$R_\epsilon = \frac{\lambda}{2\epsilon^2}(\ln(\tilde{\alpha}^2 + \tilde{\beta}^2) + 2\ln((1+\alpha)^2 + \beta^2) + (1-\alpha)\tilde{\alpha} + \beta\tilde{\beta}) - \frac{\mu|\boldsymbol{x}|}{\lambda\epsilon^2},$$

$$S_\epsilon = \frac{\lambda}{\epsilon^2}\left(\arg(\tilde{\alpha} + i\tilde{\beta}) + 2\arg(1+\alpha+i\beta) + \frac{1}{2}\tilde{\beta}(1-\alpha) - \frac{1}{2}\beta\tilde{\alpha}\right),$$

where

$$\tilde{\alpha} = \frac{\mu}{\lambda^2}\left(|\boldsymbol{x}| - \frac{x}{e}\right), \quad \tilde{\beta} = -\frac{\mu y\sqrt{1-e^2}}{\lambda^2 e}.$$

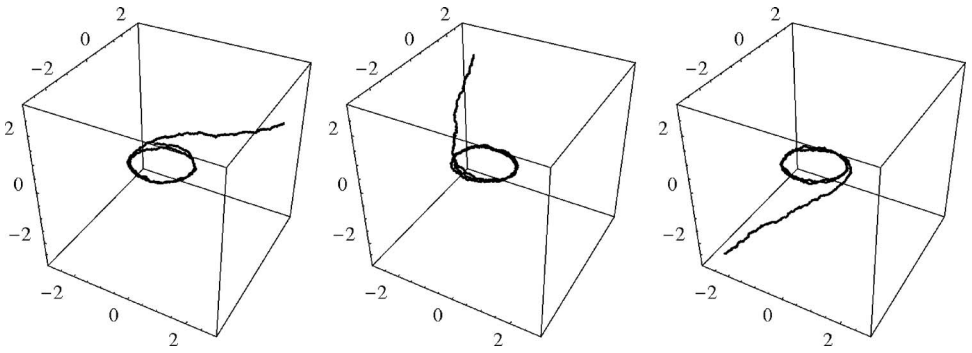

FIG. 4. Simulations of the limiting diffusion $\boldsymbol{X}^{\epsilon}$ with $e=0.5$.

Our main object of study for the rest of this paper is the limiting Nelson diffusion process $\boldsymbol{X}^{\epsilon}$ in Proposition 2. Figure 4 shows several simulations of sample paths for $\boldsymbol{X}^{\epsilon}$. These paths all converge to the Kepler ellipse. We hope to recover the Keplerian motion on the Kepler ellipse from the underlying deterministic dynamical system $\boldsymbol{X}^{0}$ found from $\boldsymbol{X}^{\epsilon}$ in the limit as $\epsilon \to 0$.

Remark 2: The process $\boldsymbol{X}^{\epsilon}$ is the formal limit of the process $\boldsymbol{X}^{\epsilon,n}$ found by letting $n \to \infty$ while $\epsilon \to 0$ with $\lambda = n\epsilon^2$ fixed, in the drift term. The process $\boldsymbol{X}^{\epsilon,n}$ before taking this limit satisfies the Nelson–Newton law

$$\frac{1}{2}(D_+D_- + D_-D_+)\boldsymbol{X}^{\epsilon,n}(t) = -\mu \frac{\boldsymbol{X}^{\epsilon,n}(t)}{|\boldsymbol{X}^{\epsilon,n}(t)|^3}.$$

C. The drift singularity

Considering Eqs. (25a) and (25b) in Proposition 2, it is clear that α and β will both have singularities at the point $|\boldsymbol{x}|=0$. However, β will also have a singularity along the surface $\alpha=0$. Therefore, the drift could be singular at any of these points.

The former is easy to analyze using spherical polar coordinates

$$x = r\cos\theta\sin\phi, \quad y = r\sin\theta\sin\phi, \quad z = r\cos\phi.$$

Then,

$$\alpha \sim C(\theta,\phi)r^{-1/2},$$

$$\beta = \frac{-2\lambda^2 e\sqrt{1-e^2}\sin\theta\sin\phi}{((e-\cos\theta\sin\phi)^2 + (1-e^2)\sin^2\theta\sin^2\phi)\mu r\alpha} \sim -K(\theta,\phi)r^{-1/2}\sin\theta\sin\phi,$$

as $r \sim 0$, where C, K are some positive functions independent of r. One would normally expect the probability of the diffusion $\boldsymbol{X}^{\epsilon}$ hitting this point singularity in finite time in two or more dimensions to be zero.

We now consider the behavior on the surface $\alpha=0$. Taking Eq. (25a), we define α_1 and α_2 so that

$$\alpha = \sqrt{\tfrac{1}{2}(\sqrt{\alpha_1} + \alpha_2)}. \tag{26}$$

Clearly, a necessary condition for $\alpha=0$ is $\alpha_1 - \alpha_2^2 = 0$, and so working in cylindrical polar coordinates

$$x = \tilde{r}\cos\theta, \quad y = \tilde{r}\sin\theta, \quad z = z,$$

we have

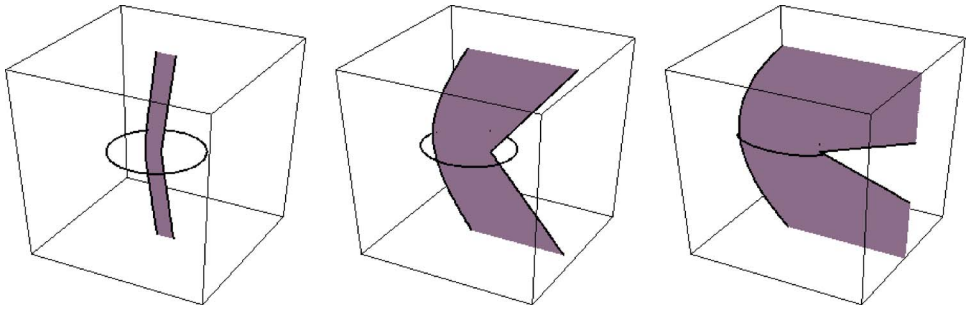

FIG. 5. (Color online) The drift singularity (shaded) with the Kepler ellipse for $e=0.1$, 0.5, and 0.9.

$$\alpha_1 - \alpha_2^2 = \frac{64\lambda^4 e^2(1-e)(e+1)\tilde{r}^2 \sin^2\theta}{\mu^2((e^2\cos 2\theta + e^2 + 2)\tilde{r}^2 - 4e\tilde{r}\sqrt{\tilde{r}^2+z^2}\cos\theta + 2e^2z^2)^2},$$

and so α is only zero on $y=0$. Moreover, returning to Cartesians,

$$\alpha|_{y=0} = \sqrt{\frac{1}{2}\left(\frac{4\lambda^2 e/\mu - e\sqrt{x^2+z^2}+x}{x-e\sqrt{x^2+z^2}} + \sqrt{\frac{(4\lambda^2 e/\mu - e\sqrt{x^2+z^2}+x)^2}{(x-e\sqrt{x^2+z^2})^2}}\right)}, \tag{27}$$

and so we can conclude

$$\alpha = 0 \Leftrightarrow \boldsymbol{x} = (x,y,z) \in \Sigma,$$

where Σ is the set,

$$\Sigma = \left\{(x,0,z):\ \frac{-e(4\lambda^2/\mu - \sqrt{(16\lambda^4/\mu^2 - z^2)e^2 + z^2})}{1-e^2} < x < \sqrt{\frac{e^2z^2}{1-e^2}}\right\}. \tag{28}$$

The set Σ is shown in Fig. 5 together with the Kepler ellipse. This singularity is what one would expect if we consider Σ as the correspondence limit of the nodal surfaces of the wave function $\psi_{\epsilon,n}$ (see Fig. 1). It can be shown that this singularity leads to a finite jump discontinuity in the drift.

D. Restriction to two dimensions

For the remainder of this paper, we shall restrict our wave functions $\psi_{\epsilon,n}$ and ψ_ϵ and their related diffusion processes $\boldsymbol{X}^{\epsilon,n}$ and $\boldsymbol{X}^\epsilon$ to the putative plane of motion $z=0$. We will consider the full three dimensional problem in a future paper.

Proposition 3: *If $\psi_\epsilon(x,y,z)$ is the three dimensional limiting wave function, then its restriction to the plane $z=0$ is given by*

$$\psi_\epsilon(x,y) = \nu^{\lambda/\epsilon^2}\left(1+\sqrt{1-\frac{4}{\nu}}\right)^{2\lambda/\epsilon^2}\exp\left(-\frac{\mu}{\lambda\epsilon^2}\sqrt{x^2+y^2} + \frac{\lambda\nu}{2\epsilon^2}\left(1-\sqrt{1-\frac{4}{\nu}}\right)\right),$$

where

$$\nu = \frac{\mu}{\lambda^2}\left(\sqrt{x^2+y^2} - \frac{x}{e} - \frac{iy\sqrt{1-e^2}}{e}\right).$$

Proof: We state without proof that the correspondence limit in three dimensions satisfies

$$\psi_\epsilon^{3\text{-dim}}|_{z=0} = \psi_\epsilon^{2\text{-dim}},$$

giving the result. □

Proposition 4: *The limiting Nelson diffusion process $\boldsymbol{X}^\epsilon = (X_x^\epsilon, X_y^\epsilon)$ restricted to the plane $z=0$*

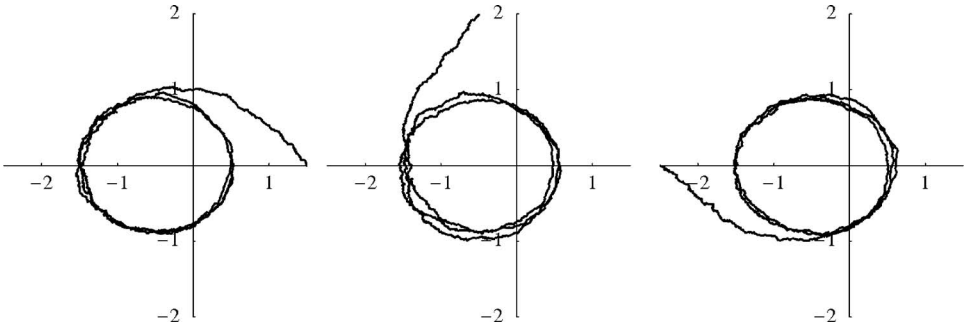

FIG. 6. Simulations of the two dimensional diffusion $\boldsymbol{X}^{\epsilon}$ for $e=0.5$.

satisfies

$$\mathrm{d}\boldsymbol{X}^{\epsilon}(s) = \boldsymbol{b}(\boldsymbol{X}^{\epsilon}(s))\mathrm{d}s + \epsilon \mathrm{d}\boldsymbol{B}(s),$$

where $\boldsymbol{b}(\boldsymbol{x})=(b_x,b_y)$ *with*

$$b_x = \frac{\mu}{2\lambda}\left\{(\alpha+\beta-1)\frac{1}{e} - (\alpha+\beta+1)\frac{x}{\sqrt{x^2+y^2}}\right\}, \tag{29a}$$

$$b_y = \frac{\mu}{2\lambda}\left\{(\alpha-\beta-1)\frac{\sqrt{1-e^2}}{e} - (\alpha+\beta+1)\frac{y}{\sqrt{x^2+y^2}}\right\} \tag{29b}$$

and

$$\alpha = \left(\frac{1}{2}\sqrt{\frac{(e\sqrt{x^2+y^2}-x-4\lambda^2 e/\mu)^2+(1-e^2)y^2}{(e\sqrt{x^2+y^2}-x)^2+(1-e^2)y^2}} + \frac{1}{2}\frac{(e\sqrt{x^2+y^2}-x-2\lambda^2 e/\mu)^2+(1-e^2)y^2-4\lambda^4 e^2/\mu^2}{(e\sqrt{x^2+y^2}-x)^2+(1-e^2)y^2}\right)^{1/2}, \tag{30a}$$

$$\beta = \frac{-2\lambda^2 e\sqrt{1-e^2}y}{\mu((e\sqrt{x^2+y^2}-x)^2+(1-e^2)y^2)\alpha}. \tag{30b}$$

Proof: This follows from Proposition 2. □

Simulations of the restricted limiting Nelson diffusion process are shown in Fig. 6.

IV. THE KEPLERIAN ELLIPTIC COORDINATE SYSTEM

In this section, we will define a new two dimensional coordinate system to simplify the limiting diffusion $\boldsymbol{X}^{\epsilon}$. Recall from Definition 1 that the Kepler ellipse is the ellipse with eccentricity e and semimajor axis $a=\lambda^2/\mu$ with one focus at the origin and the other at $(-2ae,0)$.

In the plane $z=0$, the singularity Σ defined in Eq. (28) reduces to

$$\Sigma = \left\{(x,0):\ -\frac{4ae}{1+e} < x < 0\right\}. \tag{31}$$

We want to find a coordinate system which will simplify the complex expressions α and β in Proposition 4. From Eqs. (26) and (27), it is apparent that on the singularity, α_1 becomes a perfect square. A simple calculation shows that the same also happens on the Kepler ellipse.

In fact, if we consider this square root term in polar coordinates,

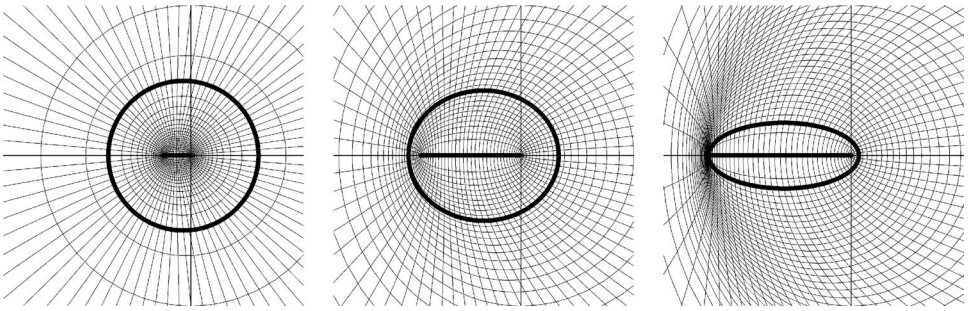

FIG. 7. The Keplerian elliptic coordinate system for $e=0.1$, 0.5, and 0.9 with the singularity ($u=1$) and Kepler ellipse ($u=e$) in bold.

$$\alpha_1 = \frac{8(2\lambda^4 - r\lambda^2\mu)e^2 + r\mu\cos\theta(8\lambda^2 - 2r\mu + er\mu\cos\theta)e + r^2\mu^2}{r^2\mu^2(e\cos\theta - 1)^2},$$

and evaluate this on an arbitrary ellipse of semimajor axis γ and eccentricity c, that is, where $r = (1-c^2)\gamma/(c\cos\theta+1)$, then we have

$$\alpha_1 = \frac{16e^2c^2\lambda^4 - 8ec\mu\lambda^2(\gamma(c^2-1) + r(ec+1)) + \mu^2(e\gamma(c^2-1) + r(c+e))^2}{(e\gamma(c^2-1) + r(c+e))^2\mu^2}.$$

The numerator is quadratic in r and so forms a perfect square when its discriminant is zero. This only occurs when $\gamma = 2ae/(c+e)$. Therefore, there is an infinite family of ellipses, including both the Kepler ellipse and the singularity (as a degenerate ellipse), on which α_1 forms a perfect square.

Definition 2: The family of ellipses $\mathcal{E}_c$ are nonconfocal ellipses with eccentricity $|c|$, foci at $(0,0)$ and $(-4aec/(1+e),0)$, and with semimajor axis $2ae/(e+c)$ where $-e \leqslant c \leqslant 1$.

Using the ellipses $\mathcal{E}_u$, we introduce (u,v) coordinates.

Definition 3: The Keplerian elliptic coordinates (u,v) in the plane (x,y) are defined by

$$x = \frac{2ae(\cos v - u)}{e+u}, \quad y = \frac{2ae\sqrt{1-u^2}\sin(v)}{e+u}, \tag{32}$$

where $-e < u \leqslant 1$ and $0 \leqslant v < 2\pi$.

These are nonorthogonal coordinates. The ellipse $\mathcal{E}_c$ corresponds to the coordinate curve $u = c$ for some constant $c \in (-e,1]$. The Kepler ellipse is the curve $u=e$ (i.e., $\mathcal{E}_e$) and the singularity is the degenerate ellipse given by $u=1$ (i.e., $\mathcal{E}_1$). The ellipse at infinity is given by $u=-e$ (i.e., $\mathcal{E}_{-e}$). The curves $v=k$ for some constant k are similar to hyperbolas. The coordinate curves are shown in Fig. 7 for several values of e. It is important to note the bunching of the curves of constant u which occurs at the left hand end of the singularity for large eccentricities.

The usefulness of Keplerian elliptic coordinates is immediately apparent as Eqs. (30a) and (30b) simplify to give

$$\alpha = \frac{\sqrt{(1-u^2)(1-e^2)}}{1+eu-(e+u)\cos v}, \quad \beta = -\frac{(e+u)\sin v}{1+eu-(e+u)\cos v}, \tag{33}$$

and the drift from Eqs. (29a) and (29b) becomes

$$b_x = \frac{\mu}{2\lambda}\left(\frac{eu-(e-u)\cos v-(e+u)\sin v+\sqrt{(1-e^2)(1-u^2)}-1}{e(1-u\cos v)}\right),$$

$$b_y = \frac{\mu}{2\lambda}\left(\frac{\sqrt{1-u^2}(e\cos v - e\sin v + 1) + \sqrt{1-e^2}(u\cos v + u\sin v - 1)}{e(1-u\cos v)}\right).$$

The singularity Σ becomes the line $u=1$ with approaches from above (i.e., $y>0$) corresponding to $0<v<\pi$ and approaches from below (i.e., $y<0$) as $\pi<v<2\pi$. In this manner, the singularity is opened out onto the boundary of our new coordinate space which forms a cylinder. It is also apparent that there is a finite jump discontinuity in β across Σ as

$$\beta|_{u=1,v=v} = -\frac{\sin v}{1-\cos v}, \quad \beta|_{u=1,v=2\pi-v} = \frac{\sin v}{1-\cos v}.$$

We can also use our new coordinates to rewrite the diffusion process $\boldsymbol{X}^\epsilon$ in (u,v) space.

Proposition 5: The diffusion $\boldsymbol{X}^\epsilon$ can be written in terms of the Keplerian elliptic coordinates (u,v) as

$$\mathrm{d}X_u^\epsilon = h(X_u^\epsilon, X_v^\epsilon)\{b_u(X_u^\epsilon, X_v^\epsilon)\mathrm{d}t - \epsilon \boldsymbol{N}(X_u^\epsilon, X_v^\epsilon)\cdot(\mathrm{d}B_1, \mathrm{d}B_2)\},$$

$$\mathrm{d}X_v^\epsilon = h(X_u^\epsilon, X_v^\epsilon)\{b_v(X_u^\epsilon, X_v^\epsilon)\mathrm{d}t - \epsilon \boldsymbol{M}(X_u^\epsilon, X_v^\epsilon)\cdot(\mathrm{d}B_1, \mathrm{d}B_2)\},$$

where

$$\boldsymbol{N}(u,v) = ((e+u)(1-u^2)\cos v, (e+u)\sqrt{1-u^2}\sin v),$$

$$\boldsymbol{M}(u,v) = ((1+eu)\sin v, -\sqrt{1-u^2}(e+\cos v)),$$

with

$$h(u,v) = \frac{(e+u)}{2ae(1-u\cos v)(eu+(e+u)\cos v+1)}$$

and

$$b_u = \epsilon^2 I_u(u,v) - \frac{\mu}{2e\lambda}(e+u)\sqrt{1-u^2}(\sqrt{1-e^2}(u+\cos v - \sin v) - \sqrt{1-u^2}(e+\cos v - \sin v)),$$

$$b_v = \epsilon^2 I_v(u,v) - \frac{\mu}{2e\lambda}(\sqrt{(1-e^2)(1-u^2)}(e+\cos v + \sin v) - u(1+e^2) - 2e - (e^2+2ue+1)\cos v - (1-e^2)\sin v),$$

with the Itô correction terms

$$I_u(u,v) = \frac{-(e+u)^2}{4ae(1+eu+(e+u)\cos v)^2}((e+u)^2((2u^2-1)\cos^2 v + 1) + 2u((e+u)^2 - (1-u^2)(1+eu))\cos v - (1-u^2)(1-e^2)),$$

$$I_v(u,v) = \frac{(e+u)\sin v}{4a(1+eu+(e+u)\cos v)^2}(2(u+e)^2 - (1+eu)^2 + (e+u)(eu+1)\cos v).$$

Proof: This follows from applying Itô's formula to Eq. (32) which defines the Keplerian elliptic coordinates. □

V. THE LIMITING NELSON DIFFUSION X^ϵ

A. The invariant measure and the infinite time limit

We want to show that the (time dependent) density $\rho_\epsilon(\boldsymbol{x},t)$ for the diffusion $\boldsymbol{X}^\epsilon$ with any given initial distribution $\rho_\epsilon^0(\boldsymbol{x})$ will converge in the infinite time limit to a density concentrated on the Kepler ellipse. We begin by showing that the invariant measure is this physically correct density in the limit as $\epsilon \to 0$.

The invariant measure for the Nelson diffusion process $\boldsymbol{X}^{\epsilon,n}$ corresponding to the atomic elliptic state wave function $\psi_{\epsilon,n}=\exp(R_{\epsilon,n}+iS_{\epsilon,n})$ is given by

$$\rho_{\epsilon,n}^\infty(\boldsymbol{x}) := \frac{\psi_{\epsilon,n}\psi_{\epsilon,n}^*}{\|\psi_{\epsilon,n}\|^2} = \frac{\exp(2R_{\epsilon,n}(\boldsymbol{x}))}{\int\int \exp(2R_{\epsilon,n}(\boldsymbol{x}))\mathrm{d}x\mathrm{d}y}.$$

This density is shown in Fig. 3 where $n=20$ and $\epsilon^2=\lambda/n$. For the limiting wave function $\psi_\epsilon=\exp(R_\epsilon+iS_\epsilon)$, the invariant measure is ρ_ϵ^∞, where

$$\rho_\epsilon^\infty(\boldsymbol{x}) := \frac{\exp(2R_\epsilon(\boldsymbol{x}))}{\int\int \exp(2R_\epsilon(\boldsymbol{x}))\mathrm{d}x\mathrm{d}y}. \tag{34}$$

Theorem 1: *The invariant density ρ_ϵ^∞ coming from the Bohr correspondence limit of the atomic elliptic state has the Kepler ellipse $\mathcal{E}_e$ as a manifold of maxima on which it attains a constant global maximum where*

$$\exp\,(2R_\epsilon(\boldsymbol{x}))\big|_{\boldsymbol{x}\in\mathcal{E}_e} = \left(\frac{16}{e^2}\right)^{\lambda/\epsilon^2}.$$

The maximum of ρ_ϵ^∞ will be sharply peaked on $\mathcal{E}_e$ as $\epsilon\to 0$.

Proof: We can write R_ϵ in terms of Keplerian elliptic coordinates (u,v) giving

$$\exp(2R_\epsilon) = 16^{\lambda/\epsilon^2}\left(\frac{1+eu+\sqrt{(1-e^2)(1-u^2)}}{e+u}\right)^{2\lambda/\epsilon^2} \times \exp\left(\frac{2a\mu(u-e+(eu-1+\sqrt{(1-e^2)(1-u^2)})\cos v)}{(e+u)\epsilon^2\lambda}\right).$$

On $\mathcal{E}_e$, this is constant,

$$\exp(2R_\epsilon(e,v)) = \left(\frac{16}{e^2}\right)^{\lambda/\epsilon^2} \Rightarrow \left.\frac{\partial}{\partial v}\exp(2R_\epsilon(u,v))\right|_{u=e} = 0.$$

Moreover, a simple calculation produces

$$\left.\frac{\partial}{\partial u}\exp(2R_\epsilon(u,v))\right|_{u=e} = 0,$$

so that $\mathcal{E}_e$ is a manifold of stationary points. A further calculation shows that this is the unique maximum for this function. Clearly, taking into account the normalization factor in ρ_ϵ^∞, the invariant density will become sharply peaked as $\epsilon\to 0$, as shown in Fig. 8. □

We now want to show that $\rho_\epsilon(\boldsymbol{x},t)$ will converge to $\rho_\epsilon^\infty(\boldsymbol{x})$ in the infinite time limit. For this, we introduce a similarity transform first developed in Ref. 19 and applicable to any Nelson diffusion $\boldsymbol{X}$ with diffusion constant $\epsilon^2/2$. The generator $\mathcal{G}$ of the diffusion $\boldsymbol{X}$ is the operator

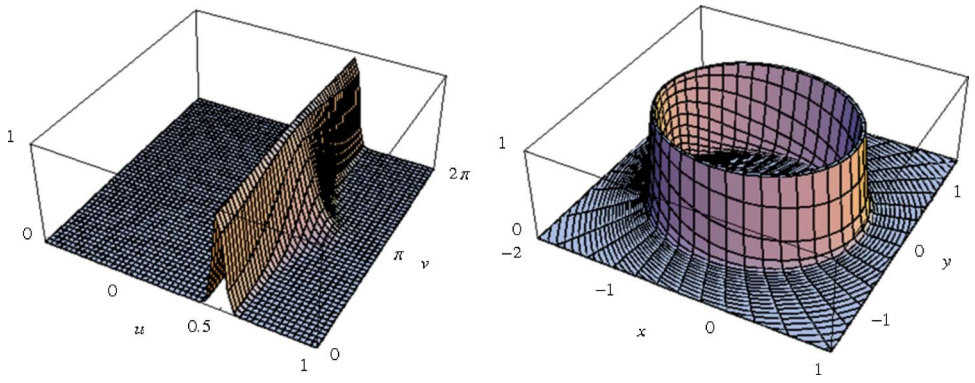

FIG. 8. (Color online) ρ_ϵ^∞ in (u,v) and (x,y) space for $e=0.5$ and $\epsilon=0.1$.

$$\mathcal{G} = \tfrac{1}{2}\epsilon^2\Delta + \boldsymbol{b}\cdot\nabla,$$

where $\boldsymbol{b}=\epsilon^2\nabla(R+S)$ for suitable real functions R and S such that the corresponding wave function can be written as $\psi=\exp(R+iS)$.

Lemma 2: For the generator $\mathcal{G}$ of a Nelson diffusion process $\boldsymbol{X}$ with diffusion constant $\epsilon^2/2$,

$$\mathcal{G} = \exp(-(R+S))(-\tilde{H}/\epsilon^2)\exp(R+S),$$

where $\tilde{H}$ is the formal Hamiltonian

$$\tilde{H} = \tfrac{1}{2}(-\epsilon^4\Delta + \boldsymbol{b}^2 + \epsilon^2\nabla\cdot\boldsymbol{b}),$$

and $\boldsymbol{b}=\epsilon^2\nabla(R+S)$. Moreover, for $\tilde{\psi}=\exp(R-S)$,

$$\tilde{H}\tilde{\psi} = 0,$$

so that $\tilde{\psi}$ is the formal ground state for $\tilde{H}$.

Proof: This follows from a calculation using the identity

$$\Delta(fg) = f\Delta g + g\Delta f + 2\nabla f\cdot\nabla g,$$

together with the real valued nature of E, V, R, and S. □

Recall that the atomic elliptic state wave function $\psi_{\epsilon,n}$ associated with the diffusion $\boldsymbol{X}^{\epsilon,n}$ is an exact solution for the Schrödinger equation. We begin by showing how for the diffusion $\boldsymbol{X}^{\epsilon,n}$ with any given initial distribution $\rho^0_{\epsilon,n}(\boldsymbol{x})$, the (time dependent) density $\rho_{\epsilon,n}(\boldsymbol{x},t)$ should converge in the infinite time limit to the invariant measure $\rho^\infty_{\epsilon,n}(\boldsymbol{x})$.

The density $\rho_{\epsilon,n}(\boldsymbol{x},t)$ satisfies the forward Kolmogorov equation (2),

$$\frac{\partial\rho_{\epsilon,n}(\boldsymbol{x},t)}{\partial t} = \mathcal{G}^*\rho_{\epsilon,n}(\boldsymbol{x},t), \quad \rho_{\epsilon,n}(\boldsymbol{x},0) = \rho^0_{\epsilon,n}(\boldsymbol{x}).$$

Therefore, using Lemma 2, we can write

$$\rho_{\epsilon,n}(\boldsymbol{x},t) = (\exp(R_{\epsilon,n}+S_{\epsilon,n})\exp(-t\tilde{H}_{\epsilon,n}/\epsilon^2)\exp(-(R_{\epsilon,n}+S_{\epsilon,n}))\rho^0_{\epsilon,n})(\boldsymbol{x}),$$

where $\tilde{H}_{\epsilon,n}=\frac{1}{2}(-\epsilon^4\Delta+\boldsymbol{b}^2_{\epsilon,n}+\epsilon^2\nabla\cdot\boldsymbol{b}_{\epsilon,n})$ is a formal Hamiltonian associated with the diffusion $\boldsymbol{X}_{\epsilon,n}$. For fixed n, the work of Blanchard and Golin[3] guarantees that with probability 1, the diffusion $\boldsymbol{X}^{\epsilon,n}$ cannot reach the nodal surfaces in a finite time because they are infinitely repulsive. Therefore, for this case, we do not need to worry about specifying a boundary condition at these points.

However, if we are to consider the case $n \to \infty$ which gives the limiting diffusion $\boldsymbol{X}^{\epsilon}$, we need to specify a boundary condition for $\rho_{\epsilon}(\boldsymbol{x},t)$ across the limiting singularity Σ. If we assume that the forward Kolmogorov equation is valid on Σ, then

$$\frac{1}{2}\mathrm{disc}_{\Sigma}\left(\epsilon^2 \frac{\partial}{\partial \boldsymbol{n}} \ln \rho_{\epsilon}(\boldsymbol{x},t)\right) = \mathrm{disc}_{\Sigma}(\boldsymbol{b}\cdot\boldsymbol{n}),$$

where $\boldsymbol{n}$ is the unit normal to the singularity Σ and disc_{Σ} is the discontinuity across Σ. The corresponding boundary condition for $\mathcal{D}(\tilde{H})$ (where $\mathcal{D}$ denotes the domain) reduces to

$$\mathrm{disc}_{\Sigma}\left(\frac{\partial \psi}{\partial y} \Big/ \psi\right) = \mathrm{disc}_{\Sigma}(b_y), \quad \psi \in \mathcal{D}(\tilde{H}).$$

The putative ground state for $\tilde{H}_{\epsilon} = \frac{1}{2}(-\epsilon^4\Delta + \boldsymbol{b}^2 + \epsilon^2 \nabla\cdot\boldsymbol{b})$ is $\tilde{\psi}_{\epsilon} = \exp(R_{\epsilon} - S_{\epsilon})$, which satisfies our boundary condition.

Assuming that there is a spectral gap, when the limiting $\tilde{H}_{\epsilon}$ is self-adjoint and satisfies this boundary condition with a genuine ground state $\tilde{\psi}_{\epsilon}$, we obtain

$$\rho_{\epsilon}(\boldsymbol{x},t) \to c_{\epsilon} \exp(2R_{\epsilon}(\boldsymbol{x})),$$

as $t \to \infty$, where

$$c_{\epsilon} = \frac{\int\int \rho_{\epsilon}^{0}(\boldsymbol{x}) \exp(-2S_{\epsilon}(\boldsymbol{x}))\mathrm{d}x\mathrm{d}y}{\int\int \exp(2(R_{\epsilon} - S_{\epsilon})(\boldsymbol{x}))\mathrm{d}x\mathrm{d}y}.$$

This suggests that the Kepler ellipse emerges in the infinite time limit.

B. The limiting diffusion as $\epsilon \to 0$

Using the methods of Veretennikov[20] and Blanchard and Golin,[3] we can prove the existence and uniqueness of solutions to the Itô stochastic differential equations defining the limiting Nelson diffusion $\boldsymbol{X}^{\epsilon}$ even though it has a singular drift field. However, we cannot easily control the limit of $\boldsymbol{X}^{\epsilon}$ as $\epsilon \to 0$.

We must therefore restrict $\boldsymbol{X}^{\epsilon}$ to sample paths avoiding the singularity Σ. We do this by estimating the probability that up to a fixed time t the process $\boldsymbol{X}^{\epsilon}(s)$ avoids the interior of a small ellipse surrounding the singularity. Then, using the methods of Freidlin and Wentzell,[10] we show how to obtain the underlying deterministic system $\boldsymbol{X}^{0}$ as the limit of $\boldsymbol{X}^{\epsilon}$ as $\epsilon \to 0$.

Definition 4: For small $\delta > 0$, define the first hitting time

$$\tau_{\boldsymbol{x}}(\mathrm{int}(\mathcal{E}_{1-\delta})) = \inf\{s > 0 : \boldsymbol{X}^{\epsilon}(s) \in \mathrm{int}(\mathcal{E}_{1-\delta}), \boldsymbol{X}^{\epsilon}(0) = \boldsymbol{x}\},$$

where $\mathcal{E}_{1-\delta}$ is a small ellipse which surrounds the singularity $\mathcal{E}_1$.

Since $\mathrm{int}(\mathcal{E}_{1-\delta})$ is open, it follows that

$$\mathbb{P}\{\tau_{\boldsymbol{x}}(\mathrm{int}(\mathcal{E}_{1-\delta})) > t\} = \lim_{\kappa \uparrow \infty} \mathbb{E}\left\{-\kappa \int_0^t \chi(\mathrm{int}(\mathcal{E}_{1-\delta}))(\boldsymbol{X}^{\epsilon}(s))\mathrm{d}s\right\}.$$

Moreover, for $\boldsymbol{x} \in \mathrm{ext}(\mathcal{E}_{1-\delta})$, the drift $\boldsymbol{b}(\boldsymbol{x})$ is Lipschitz continuous in space. The similarity transform in Lemma 2 leads naturally to the following conjecture for small ϵ^2.

Conjecture 1:

$$\mathbb{P}\{\tau_{\boldsymbol{x}}(\mathrm{int}(\mathcal{E}_{1-\delta})) > t\} \approx \exp(-(R_{\epsilon} + S_{\epsilon}))(\exp(-t\tilde{H}_{\epsilon}^{D}/\epsilon^2)\exp(R_{\epsilon} + S_{\epsilon}))(\boldsymbol{x}),$$

where

$$\tilde{H}_\epsilon^D = \lim_{\kappa\uparrow\infty}(\tilde{H}_\epsilon + \kappa\chi(\mathrm{int}(\mathcal{E}_{1-\delta})))$$

is the Dirichlet Hamiltonian with Dirichlet boundary conditions on ellipse $\mathcal{E}_{1-\delta}$, *with*

$$\tilde{H}_\epsilon = \tfrac{1}{2}(-\epsilon^4\Delta + \epsilon^2\nabla\cdot\boldsymbol{b} + \boldsymbol{b}^2),$$

for $\boldsymbol{b}=\epsilon^2\nabla(R_\epsilon+S_\epsilon)$, $\tilde{H}_\epsilon$ *being the self-adjoint extension of* $\tilde{H}_\epsilon$ *with domain* $C_0^\infty(\mathbb{R}^2\backslash\Sigma)$.

For our desired result, we want there to be a spectral gap for $\tilde{H}_\epsilon^D$. In this connection, it is worth noting that if $\nabla\cdot\boldsymbol{b}$ is bounded below and $\boldsymbol{b}^2$ has a unique global minimum at $\boldsymbol{x}_{\min}$, then

$$\tilde{H}_\epsilon \sim \tfrac{1}{2}(-\epsilon^4\Delta + \epsilon^2\nabla\cdot\boldsymbol{b}(\boldsymbol{x}_{\min}) + \boldsymbol{b}^2),$$

and according to a celebrated result of Simon,[15–18] $\sigma(\tilde{H}_\epsilon/\epsilon^2)\sim\sigma(H_0)$, where

$$H_0 = \frac{1}{2}\Delta + \frac{1}{2}\frac{\partial^2\tilde{V}}{\partial x_i\partial x_j}(\boldsymbol{x}-\boldsymbol{x}_{\min})_i(\boldsymbol{x}-\boldsymbol{x}_{\min})_j + \frac{1}{2}\nabla\cdot\boldsymbol{b}(\boldsymbol{x}_{\min}) + \tilde{V}(\boldsymbol{x}_{\min}),$$

with $\tilde{V}=\boldsymbol{b}^2/2$.

For the limiting diffusion $\boldsymbol{X}^\epsilon$,

$$\nabla_x\cdot\boldsymbol{b} = \frac{\mu(e+u)(eu+(e+u)(\cos v+\sin v)+\sqrt{(1-e^2)(1-u^2)}+1)}{4ae\lambda(u\cos v-1)(eu+(e+u)\cos v+1)} \tag{35}$$

(where $-e<u<1$) and

$$\boldsymbol{b}^2 = \frac{\mu(e\cos v+1)(\sqrt{(1-e^2)(1-u^2)}-1)}{ae^2(u\cos v-1)}. \tag{36}$$

Moreover, from Eq. (36), $\boldsymbol{b}^2$ is symmetric about the y axis ($v\mapsto -v$) and so is continuous across the singularity Σ excluding the point $|\boldsymbol{x}|=0$. It can be shown that in polar coordinates, $\boldsymbol{b}^2=\mathrm{O}(r^{-1/2})$ as $r\sim 0$ uniformly for $\theta\in(0,2\pi)$ and also that $\boldsymbol{b}^2$ has a unique global minimum when $u=e^2/(2-e^2)$ and $v=\pi$ corresponding to the point,

$$\boldsymbol{x}_{\min} = \left(\frac{-4a}{(1+e)(2-e)},0\right),$$

at which

$$\boldsymbol{b}^2(\boldsymbol{x}_{\min}) = (1-e)\frac{\mu}{2a}.$$

However, from Eq. (35), it can be shown that $\nabla\cdot\boldsymbol{b}$ is not so well behaved. It has a jump discontinuity across Σ (where $u=1$) and also blows up at each end of Σ (where $v=0$ and $v=\pi$). Firstly, in polar coordinates, $r\nabla\cdot\boldsymbol{b}\to -1$ as $r\to 0$ uniformly in θ but also $|\nabla\cdot\boldsymbol{b}|\sim r_q^{-1/2}$ as $r_q\to 0$ but not uniformly in θ, where $r_q=|\boldsymbol{x}-(-4ae/(1+e),0)|$, meaning that the divergence is not bounded below at the points $(x,y)=(-4ae/(1+e),0)$ and $(x,y)=(0,0)$. Nevertheless, we hope to publish a proof of the above conjecture in the near future using the above and results of Wang.[21]

Now, take a sequence of real numbers ϵ_j such that $\epsilon_j\to 0$ as $j\to\infty$. Then, define the sequence of limiting Nelson diffusions $\boldsymbol{X}^{\epsilon_j}$ by

$$\mathrm{d}\boldsymbol{X}^{\epsilon_j}(s) = \boldsymbol{b}(\boldsymbol{X}^{\epsilon_j}(s))\mathrm{d}s + \epsilon_j\mathrm{d}\boldsymbol{B}(s), \quad s\in(0,t), \quad \boldsymbol{X}^{\epsilon_j}(0)=\boldsymbol{x}$$

and the process $\boldsymbol{X}^0$ by

$$\mathrm{d}\boldsymbol{X}^0(s) = \boldsymbol{b}(\boldsymbol{X}^0(s))\mathrm{d}s, \quad s \in (0,t), \quad \boldsymbol{X}^0(0) = \boldsymbol{x}, \tag{37}$$

where $\boldsymbol{b}$ is as in Eqs. (29a) and (29b). Set

$$A_t^j = \{\omega\colon\ \tau_x^j(\mathrm{int}(\mathcal{E}_{1-\delta})) > t\},$$

where τ_x^j is the first hitting time for $\boldsymbol{X}^{\epsilon_j}$. Then, we have the following result which is essentially due to Freidlin and Wentzell.[10]

Theorem 2: *If* $\Sigma\epsilon_j^2 < \infty$, *then*

$$\mathbb{P}\{\boldsymbol{X}^{\epsilon_j}(s) \to \boldsymbol{X}^0(s), j \to \infty, \textit{uniformly } s \in (0,t) | A_t^j\} = 1.$$

Proof: By definition,

$$\boldsymbol{X}^{\epsilon_j}(u) - \boldsymbol{X}^0(u) = \int_0^u (\boldsymbol{b}(\boldsymbol{X}^{\epsilon_j}(s)) - \boldsymbol{b}(\boldsymbol{X}^0(s)))\mathrm{d}s + \epsilon_j \boldsymbol{B}(u), \quad u \in (0,t).$$

If we restrict $\omega \in A_t^j$, then for some Lipschitz constant $K > 0$,

$$|\boldsymbol{X}^{\epsilon_j}(u) - \boldsymbol{X}^0(u)| \leqslant K\int_0^u |\boldsymbol{X}^{\epsilon_j}(s) - \boldsymbol{X}^0(s)|\mathrm{d}s + \epsilon_j|\boldsymbol{B}(u)|.$$

Set

$$f(t) = \int_0^t |\boldsymbol{X}^{\epsilon_j}(u) - \boldsymbol{X}^0(u)|\mathrm{d}u,$$

then

$$\dot{f}(u) = |\boldsymbol{X}^{\epsilon_j}(u) - \boldsymbol{X}^0(u)| \leqslant Kf(u) + \epsilon_j|\boldsymbol{B}(u)|, \quad u \in (0,t).$$

Therefore,

$$\frac{\mathrm{d}}{\mathrm{d}u}(\exp(-Ku)f(u)) \leqslant \epsilon_j \exp(-Ku)|\boldsymbol{B}(u)|$$

and so

$$f(s) \leqslant \epsilon_j \exp(Ks)\int_0^s \exp(-Ku)|\boldsymbol{B}(u)|\mathrm{d}u,$$

$$\dot{f}(s) \leqslant \epsilon_j K \exp(Ks)\int_0^s \exp(-Ku)|\boldsymbol{B}(u)|\mathrm{d}u + \epsilon_j|\boldsymbol{B}(s)|.$$

Therefore,

$$\sup_{s\in(0,t)} |\boldsymbol{X}^{\epsilon_j}(u) - \boldsymbol{X}^0(u)| \leqslant 3\epsilon_j \sup_{s\in(0,t)} |\boldsymbol{B}(u)|.$$

For any constant $c > 0$,

$$\mathbb{P}\{\sup_{s\in(0,t)} |\boldsymbol{X}^{\epsilon_j}(u) - \boldsymbol{X}^0(u)| > c\} \leqslant \mathbb{P}\left\{\sup_{s\in(0,t)} |\boldsymbol{B}(u)| > \frac{c}{3\epsilon_j}\right\} \leqslant 2\exp\left(-\frac{c^2}{18\epsilon_j^2 t}\right).$$

Therefore, since $\exp(-x) < x^{-1}$ for $x > 0$, for any $c > 0$,

$$\sum_j \mathbb{P}\{\sup_{s\in(0,t)} |\boldsymbol{X}^{\epsilon_j}(u)-\boldsymbol{X}^0(u)|>c\} \leqslant \frac{36t}{c^2}\sum_j \epsilon_j^2 < \infty.$$

The result now follows from the Borel–Cantelli lemma. □

The last result is vacuous unless $\mathbb{P}\{A_t^j\}>0$. We can estimate this probability with Jensen's inequality, giving

$$\mathbb{E}\left\{\exp\left(-\kappa\int_0^t \chi(\mathrm{int}(\mathcal{E}_{1-\delta}))(\boldsymbol{X}_s^{\epsilon_j})\mathrm{d}s\right)\right\} \geqslant \exp\left(-\kappa\mathbb{E}\left\{\int_0^t \chi(\mathrm{int}(\mathcal{E}_{1-\delta}))(\boldsymbol{X}_s^{\epsilon_j})\mathrm{d}s\right\}\right).$$

If we choose δ such that the Lebesgue measure $\mathrm{Leb}(\mathrm{int}(\mathcal{E}_{1-\delta}))=h_t(\epsilon_j)\kappa^{-1}$ and let $\kappa\uparrow\infty$, then formally

$$\mathbb{P}_x\{A_t^j\} \geqslant \exp\left(-h_t(\epsilon_j)\int_0^t \mathrm{d}s \sup_{s\in(0,t)y\in\Sigma} p_s^j(\boldsymbol{x},\boldsymbol{y})\right),$$

where p_s^j is the transition density for $\boldsymbol{X}^{\epsilon_j}$ and the supremum is taken over $\boldsymbol{y}\in\Sigma^{\pm}$, the upper and lower parts of the singularity, with p_s^j possibly discontinuous across Σ.

By methods of Wang,[21] we have

$$\sup_{x,y} p_t^j(\boldsymbol{x},\boldsymbol{y}) \leqslant \frac{1}{t}\exp\left(c\left(\frac{1}{\epsilon_j^2}+\frac{t}{\epsilon_j^4}\right)\right),$$

where $\epsilon_j\in(0,1]$ and $t>0$. Then, choosing $h_t(\epsilon)=\epsilon\exp(-c/\epsilon^2)\exp(-ct/\epsilon^4)$ gives

$$\mathbb{P}\{\tau_x^j>t\}+\mathbb{P}\{\tau_x^j<\Delta\} \leqslant \left(\frac{\Delta}{t}\right)^{\epsilon}.$$

Moreover, the term $\mathbb{P}\{\tau_{\boldsymbol{x}}^j<\Delta\}$ can be made arbitrarily small compared to $\mathbb{P}\{\tau_{\boldsymbol{x}}^j>t\}$ for small Δ, giving the desired result.

VI. THE KEPLERIAN DYNAMICAL SYSTEM

A. The dynamical system and Kepler's laws of motion

In the last section, we showed that for paths avoiding the singularity, the limiting Nelson diffusion $\boldsymbol{X}^{\epsilon}$ converged to the underlying deterministic system $\boldsymbol{X}^0$ as $\epsilon\to 0$. We now consider the behavior of this deterministic system.

Definition 5: The Keplerian dynamical system is given by the equations

$$\dot{\boldsymbol{x}}=\boldsymbol{b}(\boldsymbol{x}) \Leftrightarrow \dot{x}=b_x(x,y), \quad \dot{y}=b_y(x,y),$$

where b_x and b_y are as defined in Eqs. (29a) and (29b).

The vector field for this dynamical system is shown in Fig. 9 together with the Kepler ellipse and the singularity Σ.

Remark 3: Although we use the name "dynamical system" for the differential equations in Definition 5, they do not necessarily give a system satisfying the definition of a true dynamical system (see Refs. 1 and 2 for a full definition). This is because the existence of the singularity Σ means that we cannot use the standard methods of differential equations to ascertain the existence, uniqueness, and extendability of solutions through every point of $\mathbb{R}^2$. However, as we will show, any path starting outside the Kepler ellipse will stay away from the singularity and so we can assume that the definition applied to the exterior of the Kepler ellipse will produce a dynamical system. Where necessary, we will assume that we are working solely on the exterior of $\mathcal{E}_e$. We hope to extend this work to include all paths using the work of Fillipov.[9]

We begin our anlaysis of the Keplerian dynamical system with a very simple derivation of Kepler's laws of planetary motion.

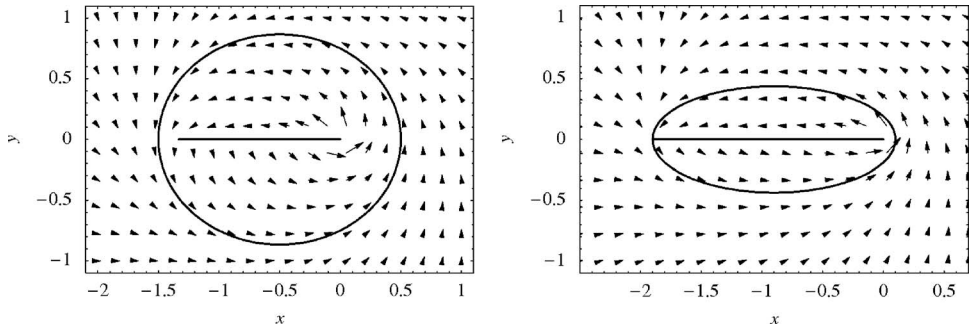

FIG. 9. The vector field of the Keplerian dynamical system with $e=0.5$ and 0.9 showing the Kepler ellipse and singularity.

Theorem 3: *The Keplerian dynamical system has the Kepler ellipse $\mathcal{E}_e$ as a periodic orbit. Moreover, a particle moving on the periodic orbit $\mathcal{E}_e$ obeys Kepler's laws of motion with force constant μ and energy $E=-\mu/2a$.*

Proof: Using Proposition 5, we can write the deterministic system in the Keplerian elliptic coordinates as

$$\dot{u} = b_u(u,v), \quad \dot{v} = b_v(u,v), \tag{38}$$

with $\epsilon=0$. The Kepler ellipse $\mathcal{E}_e$ has the equation $u=e$ and a simple calculation gives $b_u(e,v) \equiv 0$ so that $\mathcal{E}_e$ is a periodic orbit.

Moreover, for $u=e$, Eq. (32) which defines u and v reduces to give

$$x = a\cos v - ae, \quad y = a\sqrt{1-e^2}\sin v,$$

so that v is the eccentric angle for the ellipse $\mathcal{E}_e$. Then, the equations of motion (38) reduce to

$$\dot{v} = b_v(e,v) = \frac{\mu}{\lambda a(1-e\cos v)} = \sqrt{\frac{\mu}{a^3}}\frac{1}{(1-e\cos v)},$$

which is the Kepler law of motion in terms of the eccentric angle v with force constant μ and energy $E=-\mu/2a$, where $a=\lambda^2/\mu$. □

In the following sections, we will consider the convergence of trajectories of the Keplerian dynamical system to the Kepler ellipse. In the next section, we will show which initial positions produce trajectories which avoid the singularity. In the subsequent sections, we will consider the asymptotic stability of the Kepler ellipse and we will show that all trajectories which avoid the singularity will converge to the Kepler ellipse in such a manner that they will also obey Kepler's laws in the infinite time limit.

B. Avoiding the singularity

We want to show which initial positions give rise to trajectories that avoid the singularity. For the dynamical system,

$$\dot{\boldsymbol{x}}(t) = \boldsymbol{b}(\boldsymbol{x}(t)), \quad t > t_0, \quad \boldsymbol{x}(t_0) = \boldsymbol{x}_0,$$

we denote the solution $\boldsymbol{x}(t)=\boldsymbol{x}(t;\boldsymbol{x}_0,t_0)$.

From Eq. (38), the Keplerian dynamical system can be written in Keplerian elliptic coordinates as

$$\dot{u} = b_u(u,v), \quad \dot{v} = b_v(u,v).$$

The drift b_u tells us about the motion toward and away from the singularity Σ which is given by $u=1$. Thus, we are particularly interested in the sign of b_u.

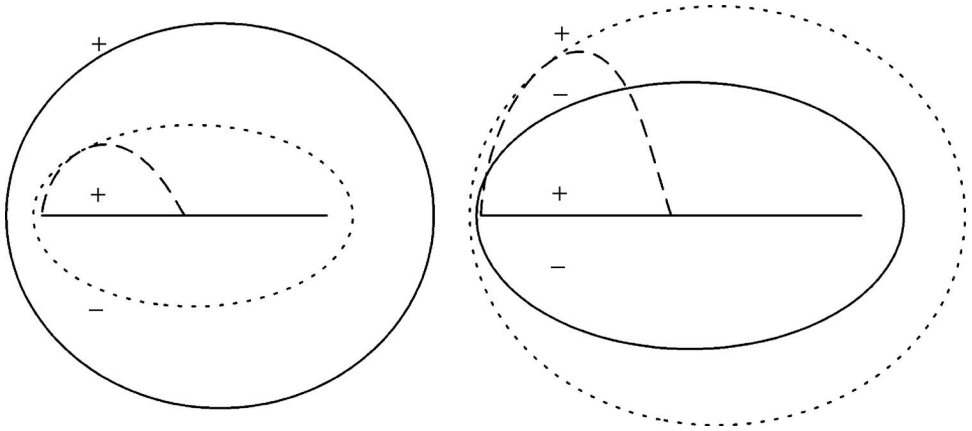

FIG. 10. The Kepler ellipse $\mathcal{E}_e$ and singularity (solid line) with the curve $u=\mathcal{F}(v)$ (dashed line), the ellipse $\mathcal{E}_{\tilde{e}}$ (dotted line), and the sign of b_u indicated.

Lemma 3: For the Keplerian dynamical system represented in Keplerian elliptic coordinates, if $u \in (-e,1)$,

$$b_u = 0 \Leftrightarrow \begin{cases} u = e, & v \in (0,2\pi) \\ u = \mathcal{F}(v), & v \in (\pi/2,\pi), \end{cases}$$

where $\mathcal{F}(v)=\mathcal{F}_{(e,1)}(v)/\mathcal{F}_{(-1,-e)}(v)$ *and*

$$\mathcal{F}_{(e_1,e_2)}(v) = e_1(1-\cos v \sin v) + e_2(\cos v - \sin v). \tag{39}$$

Proof: A simple calculation from Proposition 5. The curve $u=\mathcal{F}(v)$ is shown in the Cartesian frame in Fig. 10. □

Corollary 1: The singularity Σ *in the Cartesian plane is repulsive everywhere except for*

$$-\frac{4ae}{1+e} \leqslant x \leqslant -\frac{2ae}{1+e},$$

where for $y>0$ *the singularity is attractive.*

Proof: For $u=1$, $b_u>0$ for $v \in (\pi/2,\pi)$ but $b_u<0$ for all other v. □

Corollary 1 shows that paths which start away from the singularity may reach it in a finite time. Using Lemma 3, we can identify which initial positions may lead to this behavior. It can be shown that the curve $u=\mathcal{F}(v)$ reaches its minimum at $v=3\pi/4$ and its maximum at $v=\pi/2$ and $v=\pi$. Therefore,

$$1 > \mathcal{F}(v) > \tilde{e} \quad \text{where } \tilde{e} := \frac{-2\sqrt{2}+3e}{-3+2\sqrt{2}e}.$$

Corollary 2: If $\boldsymbol{x}_0 \in \mathrm{ext}(\mathcal{E}_e) \cup \mathrm{ext}(\mathcal{E}_{\tilde{e}})$, *then* $\boldsymbol{x}(t;\boldsymbol{x}_0,t_0)$ *will never reach the singularity for* $t > t_0$.

This tells us that outside an ellipse surrounding the singularity $\Sigma=\mathcal{E}_1$, the trajectories of the dynamical system will not intersect Σ. The ellipses $\mathcal{E}_e$ and $\mathcal{E}_{\tilde{e}}$ are shown in Fig. 10.

Remark 4: From this we can conclude the following (see Fig. 10).

(1) For $e=1/\sqrt{2}$, it follows that $\tilde{e}=1/\sqrt{2}$ so that $\mathcal{E}_e=\mathcal{E}_{\tilde{e}}$.
(2) For $e<1/\sqrt{2}$, it follows that $1>\tilde{e}>e$ so that $\mathcal{E}_e \subset \mathrm{ext}(\mathcal{E}_{\tilde{e}})$.
(3) For $e>1/\sqrt{2}$, it follows that $-e<\tilde{e}<e$ so that $\mathcal{E}_{\tilde{e}} \subset \mathrm{ext}(\mathcal{E}_e)$.

C. The asymptotic stability of Keplerian motion

We will now look at the attraction of paths which avoid the singularity to the Keplerian orbit and also at the stability of this orbit.

Definition 6: A periodic orbit generating a closed trajectory C is called orbitally stable if for any $\delta_1>0$ and any initial position $\boldsymbol{x}_0$, which yields a periodic solution traversing C, there exists $\delta_2>0$ such that

$$|\tilde{\boldsymbol{x}}_0-\boldsymbol{x}_0|<\delta_2 \Rightarrow d(\boldsymbol{x}(t;\tilde{\boldsymbol{x}}_0,t_0),C)<\delta_1,$$

for $t>t_0$, where d denotes the metric $d(\boldsymbol{x},C)=\inf|\boldsymbol{x}-\boldsymbol{y}|$ for $\boldsymbol{y}\in C$.

Moreover, if there also exists a $\delta_3>0$ such that

$$|\tilde{\boldsymbol{x}}_0-\boldsymbol{x}_0|<\delta_3 \Rightarrow \lim_{t\to\infty} d(\boldsymbol{x}(t;\tilde{\boldsymbol{x}}_0,t_0),C)=0,$$

then the orbit is said to be asymptotically orbitally stable.

For a two dimensional system, we have the following result.[22]

Theorem 4: *The closed trajectory C corresponding to a periodic solution $\boldsymbol{x}_p(t)$ of period T of a dynamical system is asymptotically orbitally stable if*

$$\int_0^T \mathrm{Tr}\left(\left.\frac{\partial \boldsymbol{b}}{\partial \boldsymbol{x}}(\boldsymbol{x})\right|_{\boldsymbol{x}=\boldsymbol{x}_p(t)}\right)\mathrm{d}t<0.$$

Theorem 5: *For the Keplerian dynamical system, let $\boldsymbol{x}_p(t)$ be a periodic trajectory traversing the Kepler ellipse $\mathcal{E}_e$ with period $T=2\pi\sqrt{a^3/\mu}$. Then,*

$$\int_0^T \mathrm{Tr}\left(\left.\frac{\partial \boldsymbol{b}}{\partial \boldsymbol{x}}(\boldsymbol{x})\right|_{\boldsymbol{x}=\boldsymbol{x}_p(t)}\right)\mathrm{d}t=-2\pi.$$

Proof: We can calculate this integral using Keplerian elliptic coordinates,

$$\begin{aligned}\int_0^T \mathrm{Tr}\left(\left.\frac{\partial \boldsymbol{b}}{\partial \boldsymbol{x}}(\boldsymbol{x})\right|_{\boldsymbol{x}=\boldsymbol{x}_p(t)}\right)\mathrm{d}t &= \int_0^{2\pi}\left\{\frac{1}{b_v}\left(\frac{\partial b_x}{\partial x}+\frac{\partial b_y}{\partial y}\right)\right\}_{u=e}\mathrm{d}v=-\int_0^{2\pi}\frac{e\cos v+e\sin v+1}{e^2+2e\cos v+1}\mathrm{d}v\\ &=-2\int_0^{\pi}\frac{e\cos v+1}{e^2+2e\cos v+1}\mathrm{d}v=-\lim_{v\uparrow\pi}\left(v+2\tan^{-1}\left(\frac{1-e}{1+e}\tan\left(\frac{v}{2}\right)\right)\right)\\ &=-2\pi,\end{aligned}$$

as $1>e>0$. □

Corollary 3: The Kepler ellipse $\mathcal{E}_e$ is an asymptotically orbitally stable periodic orbit for the Keplerian dynamical system.

We can also demonstrate that the Kepler ellipse is asymptotically orbitally stable by using the invariant density ρ_ϵ^∞ from Eq. (34) as a Lyapunov function.

Theorem 6: *Let $V_{\mathrm{Lpv}}(\boldsymbol{x})$ be a real valued function defined in an open neighborhood $N(C)$ of a compact set C. Assume that*

(1) *$V_{\mathrm{Lpv}}(\boldsymbol{x})$ is continuously differentiable,*
(2) *$V_{\mathrm{Lpv}}(\boldsymbol{x})$ is positive definite in $N(C)\backslash C$, and*
(3) *$\nabla V_{\mathrm{Lpv}}(\boldsymbol{x})\cdot\boldsymbol{b}(\boldsymbol{x})$ is negative definite in $N(C)\backslash C$, and*
(4) *$V_{\mathrm{Lpv}}(\boldsymbol{x})=\nabla V_{\mathrm{Lpv}}(\boldsymbol{x})\cdot\boldsymbol{b}(\boldsymbol{x})=0$ for $\boldsymbol{x}\in C$.*
Then the compact set C is asymptotically stable.

The function V_{Lpv} in Theorem 6 is called a Lyapunov function.

Theorem 7: *The function*

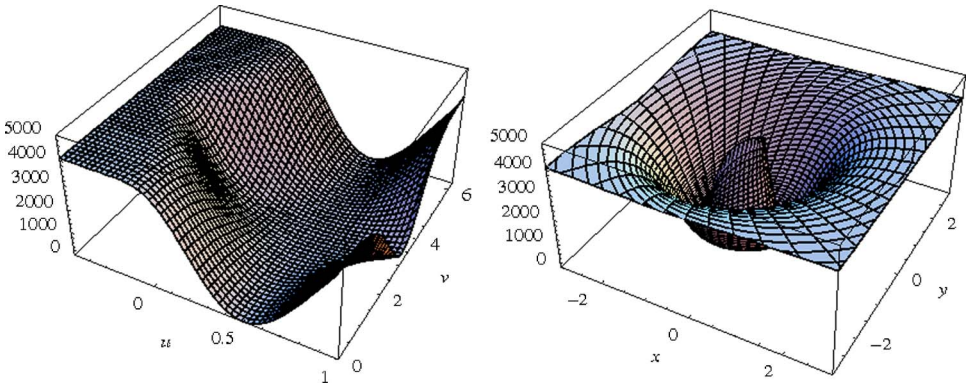

FIG. 11. (Color online) The Lyapunov function V_{Lpv} in (u,v) and (x,y) coordinates for $e=0.5$.

$$V_{\mathrm{Lpv}} = (16/e^2)^{\lambda} - \exp(2R_{\epsilon})|_{\epsilon=1}$$

satisfies the conditions of Theorem 6 for the compact set $C=\mathcal{E}_e$ *and the neighborhood* $N(C)=\mathrm{int}(\mathcal{E}_{-e+\delta_1})\backslash\mathrm{int}(\mathcal{E}_{1-\delta_2})$ *for any* $\delta_1,\delta_2\in(0,1+e)$ *such that* $\delta_1+\delta_2<1+e$.

Proof: This follows simply from Theorem 1. The function V_{Lpv} is shown in Fig. 11. It is continuous but is not smooth across Σ. The derivative $\nabla V_{\mathrm{Lpv}}\cdot\boldsymbol{b}$ is shown in Fig. 12. We exclude the ellipse at infinity $\mathcal{E}_{-e}$, as the derivative is zero in the limit. □

Asymptotic orbital stability tells us that not only does any trajectory sufficiently close to $\mathcal{E}_e$ converge in the large time limit to $\mathcal{E}_e$ but that in this large time limit, any converging trajectory will move exactly as a trajectory on $\mathcal{E}_e$. Therefore, the motion of a particle which converges toward the ellipse $\mathcal{E}_e$ must converge to the Keplerian motion on $\mathcal{E}_e$.

D. Region of attraction to the Kepler ellipse

We now look at which initial positions produce trajectories which are attracted to the Kepler ellipse in the infinite time limit. As in Sec. VI B, we are particularly interested in the sign of b_u as the Kepler ellipse is given by the coordinate curve $u=e$ and we know that $b_u=0$ on this curve.

Theorem 8: *Let* $0<e<\frac{1}{\sqrt{2}}$. *For any initial position* $\boldsymbol{x}_0\in\mathrm{ext}(\mathcal{E}_{\tilde{e}})$ *and any given* $\delta>0$, *there exists a finite time* $T>0$ *such that*

$$d(\boldsymbol{x}(t;\boldsymbol{x}_0,t_0),\mathcal{E}_e)<\delta,$$

for all times $t>T$.

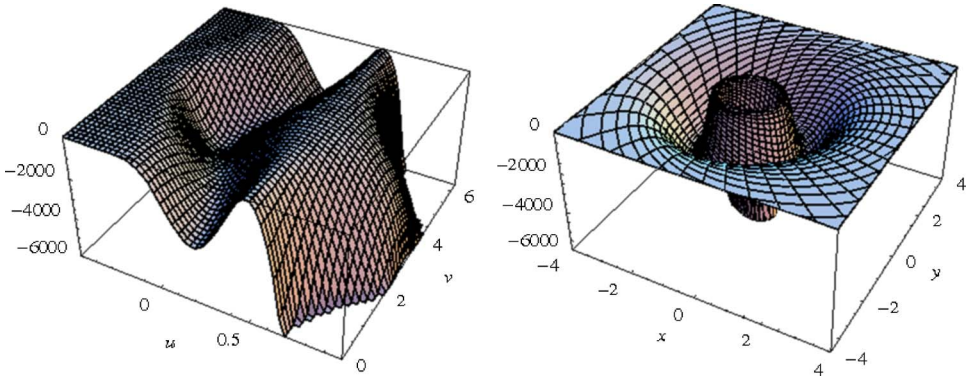

FIG. 12. (Color online) The derivative $\nabla_x V_{\mathrm{Lpv}}\cdot\boldsymbol{b}(\boldsymbol{x})$ in (u,v) and (x,y) coordinates for $e=0.5$.

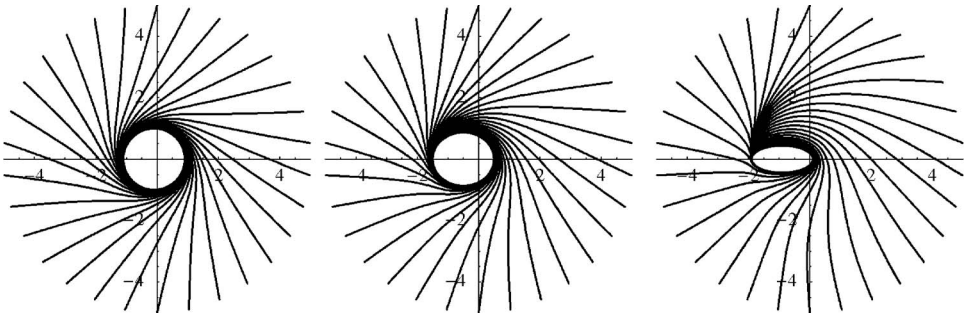

FIG. 13. Simulations of the Keplerian dynamical system with $e=0.1$, 0.5, and 0.9.

Proof: For the curve $u=\mathcal{F}(v)$ to cut the Kepler ellipse $u=e$, we would require $e<\tilde{e}$ or equivalently $e<\frac{1}{\sqrt{2}}$. Therefore, if $0<e<\frac{1}{\sqrt{2}}$, then (as shown in Fig. 10)

(1) for $-e<u<e$, $b_u>0$, and
(2) for $e<u\leqslant\mathcal{F}(v)$, $b_u<0$.

Since $\boldsymbol{b}^2>0$ for all $u\in(-e,1)$ and $v\in[0,2\pi)$, the result follows. □

From the proof of Theorem 8, we see that for $0<e<\frac{1}{\sqrt{2}}$, the Kepler ellipse is a stable orbit in the (u,v) frame as the curve $u=\mathcal{F}(v)$ does not intersect the Kepler ellipse. However, when $e=\frac{1}{\sqrt{2}}$, the curve $u=\mathcal{F}(v)$ touches the Kepler ellipse, and for $e>\frac{1}{\sqrt{2}}$, it intersects the Kepler ellipse. Thus, there is a portion of the Kepler ellipse which is unstable in this frame. Despite this, we cannot conclude that the Kepler ellipse will be unstable in the Cartesian frame as the properties of stability and instability are not necessarily coordinate invariant. As we showed in Corollary 3, the Kepler ellipse is actually stable. As can be seen in Fig. 13, simulations of the dynamical system starting outside the Kepler ellipse always converge to the ellipse. The region bounded by the curve $u=\mathcal{F}(v)$ is where this convergence is particularly slow. It would seem sensible to investigate whether $e=\frac{1}{\sqrt{2}}$ is a critical value of the eccentricity. It could be that this apparent instability is a property of the (u,v) coordinate system. As we shall see in the next section, this is not the case!

If we assume $e<\frac{1}{\sqrt{2}}$, then we can avoid these problems, and combining our results we can conclude the following.

Theorem 9: *For $0<e<\frac{1}{\sqrt{2}}$, any orbit of our Keplerian dynamical system with a start point outside the ellipse $\mathcal{E}_{\tilde{e}}$ settles down in the infinite time limit to the Keplerian motion on the Kepler ellipse $\mathcal{E}_e$.*

Proof: This follows from the asymptotic stability combined with Theorems 3 and 8. The region of convergence is shown in Fig. 14(a). □

We now consider ways to extend this domain of attraction to include eccentricities $e>\frac{1}{\sqrt{2}}$. Arguing exactly as above, we have the following result which restricts the location of the trajectory after a finite time to a large neighborhood of the Kepler ellipse.

Theorem 10: *Let $1>e>\frac{1}{\sqrt{2}}$. For any initial position $\boldsymbol{x}_0\in\mathrm{ext}(\mathcal{E}_e)$, there exists a finite time $T>0$ such that*

$$\boldsymbol{x}(t;\boldsymbol{x}_0,t_0)\in\mathrm{int}(\mathcal{E}_{\tilde{e}})\cap\mathrm{ext}(\mathcal{E}_e),$$

for all times $t>T$.

Proof: The same as that for Theorem 8, but now $\tilde{e}>e$ so that $\mathcal{E}_e\subset\mathcal{E}_{\tilde{e}}$. This region is shown in Fig. 14(b). □

This still leaves us to prove that trajectories in this elliptic annulus converge to the Kepler ellipse. This can be done using the Lyapunov function in Theorem 7 and results of Ref. 1.

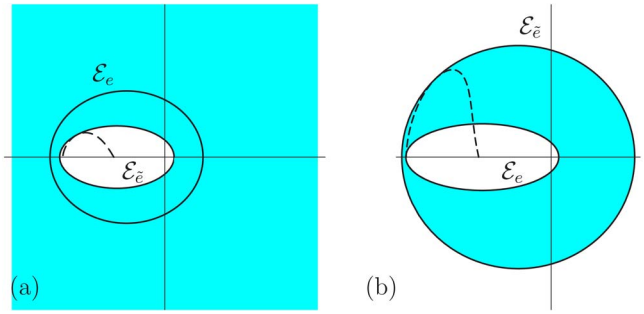

FIG. 14. (Color online) Theorems 9 and 10. (a) The region of attraction (shaded) for $\mathcal{E}_e$ with $e<\frac{1}{\sqrt{2}}$. (b) For $e>\frac{1}{\sqrt{2}}$, any trajectory starting outside the Kepler ellipse must converge to somewhere in the shaded region.

E. Surprising symmetries and mild instabilities

The appearance of $e=\frac{1}{\sqrt{2}}$ as an important eccentricity could easily be dismissed as a property of the Keplerian elliptic coordinate system. Numerical experiments confirm that although b_u does switch sign in a neighborhood of the Kepler ellipse for $e>\frac{1}{\sqrt{2}}$, the test particle always moves toward the Kepler ellipse in this region. This discrepancy can be explained easily by considering the bunching of level surfaces of u which occurs in the Keplerian elliptic coordinates (see Fig. 7) and also the slow rate of convergence in this region (see Fig. 13), particularly for large eccentricities. It is therefore surprising to encounter this critical eccentricity through other calculations.

Recall that if $u\neq e$, then

$$b_u=0\Leftrightarrow u=\frac{\mathcal{F}_{(e,1)}(v)}{\mathcal{F}_{(-1,-e)}(v)},\quad v\in(\pi/2,\pi),$$

where $\mathcal{F}_{(e_1,e_2)}(v)$ is as defined in Eq. (39).

If we consider the divergence of the drift field calculated in Cartesians but presented in Keplerian elliptic coordinates for simplicity [see Eq. (35)], then we find

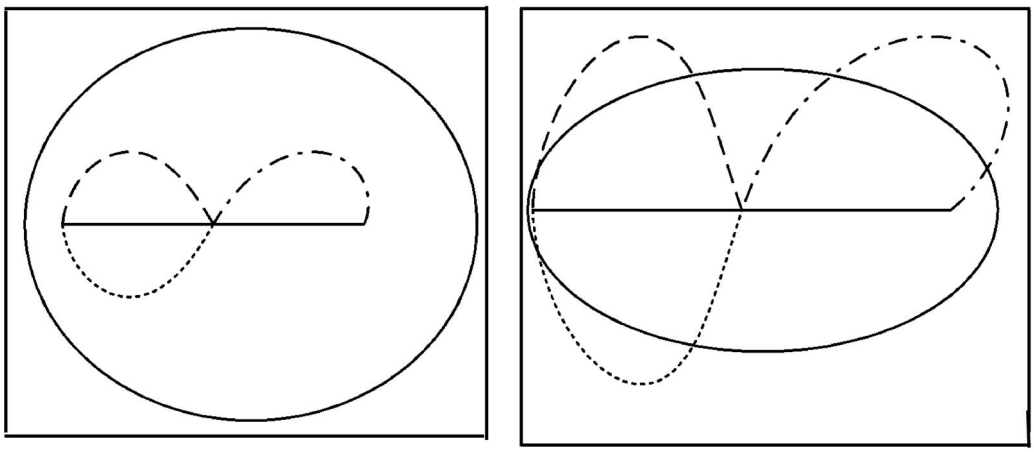

FIG. 15. The curves $b_u=0$ (long dash), $\nabla\cdot\boldsymbol{b}=0$ (dotted), and $\alpha+\beta+1=0$ (dash-dot line) with the Kepler ellipse and singularity for $e=0.5$ and 0.8.

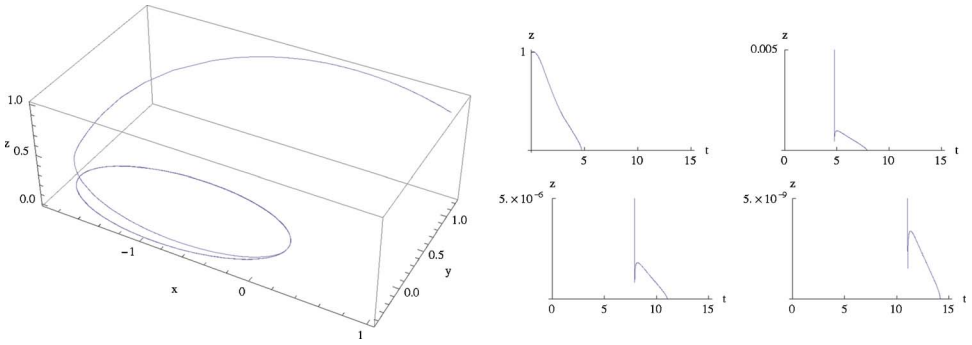

FIG. 16. (Color online) Simulation for $\epsilon=0$ and $e=0.9$ highlighting the periodic blips in z.

$$\nabla \cdot \boldsymbol{b} = 0 \Leftrightarrow u = \frac{\mathcal{F}_{(e,1)}(-v)}{\mathcal{F}_{(-1,-e)}(-v)}, \quad v \in (\pi, 3\pi/2).$$

Therefore, the curve $\nabla\cdot\boldsymbol{b}=0$ is the reflection in the y axis of the curve $b_u=0$. Moreover, this leads to the conclusion that for $e<\frac{1}{\sqrt{2}}$, the curve $\nabla\cdot\boldsymbol{b}=0$ does not cut the Kepler ellipse, and so on all parts of the ellipse $\nabla\cdot\boldsymbol{b}<0$. However, for $e>\frac{1}{\sqrt{2}}$, there is a portion of the ellipse where $\nabla\cdot\boldsymbol{b}>0$, suggesting a local mild instability in this region.

These instabilities are not just properties of the two dimensional restriction. If we consider the full three dimensional system, then the drift in the z direction is given by

$$b_z = -\frac{\mu}{2\lambda}(\alpha+\beta+1)\frac{z}{|\boldsymbol{x}|}.$$

Thus, if $\alpha+\beta+1>0$, then any test particle will always be attracted toward the plane $z=0$. Let us consider the behavior of $\alpha+\beta+1$ in the plane $z=0$. Working from Eq. (33), it is simple to show that

$$\alpha+\beta+1=0 \Leftrightarrow u = \frac{\mathcal{F}_{(e,-1)}(-v)}{\mathcal{F}_{(-1,e)}(-v)}, \quad v \in (0, \pi/2),$$

which is a curve in the same family again. It again meets the Kepler ellipse when $e=\frac{1}{\sqrt{2}}$. Therefore, when $e>\frac{1}{\sqrt{2}}$, there will be a region of the Kepler ellipse where the orbit is unstable in the z direction, as within this curve $\alpha+\beta+1<0$ which will mean $b_z>0$ for small $z>0$ and $b_z<0$ for small $z<0$. These three curves are shown together in Fig. 15.

In fact, the curve $\alpha+\beta+1=0$ is a slice of a three dimensional surface which, together with the singularity, bounds a region of space where b_z will be directed away from the plane $z=0$. This creates a general instability in orbits for $e>\frac{1}{\sqrt{2}}$, as this region is cut by the Kepler ellipse. The effect of this in the deterministic case is shown in Fig. 16. There is a clear blip in the value of z

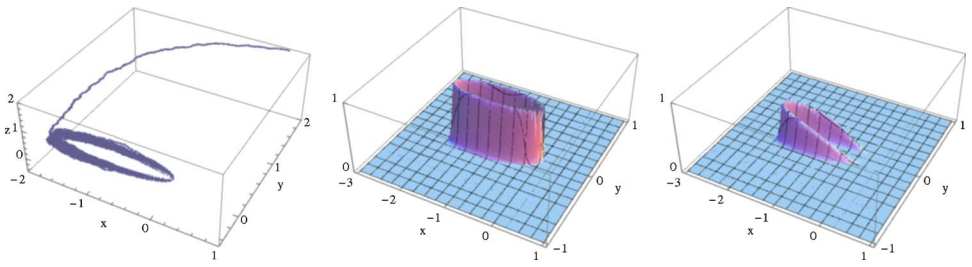

FIG. 17. (Color online) Simulation for $\epsilon=0.05$ and $e=0.99$ with the invariant measure in the planes $z=0$ and $z=0.05$.

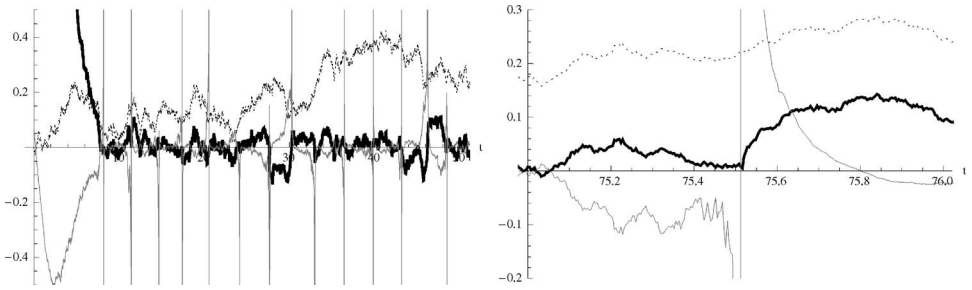

FIG. 18. The z value (thick line) with drift b_z (thin line) and driving noise B_3 (dotted line) for $\epsilon=0.05$ and $e=0.99$ with a close up of a blip.

where the particle moves away from the plane $z=0$. This blip is repeated each time the particle passes through this region, but each time the blip becomes smaller as the particle moves closer to the plane $z=0$. In the infinite time limit, the particle still appears to converge to the plane $z=0$. However, in the stochastic case ($\epsilon\neq 0$), the noise creates a displacement such that the particle never appears to settle down into a small neighborhood of the plane $z=0$ (see Figs. 17 and 18). This is caused by the presence of the noise but is apparently exacerbated by these repeated blips in b_z, which unlike the deterministic case do not decrease in magnitude in the infinite time limit (see Fig. 18). This effect becomes more pronounced as $e\to 1$ since the trajectories pass closer to the origin where $|\alpha|,|\beta|\sim r^{-1/2}$. The periodic spikes in b_z shown in Fig. 18 are the result of this effect and cause the particle to be strongly forced into the plane $z=0$ when near the point $(a-ae,0,0)$. The blip in b_z occurs immediately after the particle has passed this point, forcing it away from the plane $z=0$ again.

VII. CONCLUSIONS

We have shown that in the Bohr correspondence limit in two dimensions, the Nelson diffusion process corresponding to the atomic elliptic state for the Coulomb problem reduces to Keplerian motion on the Kepler ellipse for motions starting outside this ellipse. This solves a long standing problem in quantum mechanics. In the quantum mechanical setting, Kepler's laws of planetary motion need to be augmented with a caveat about the mild local instabilities appearing on the elliptical orbit for eccentricities greater than $\frac{1}{\sqrt{2}}$ which may be experimentally detectable. In any case, these results merit further study in the setting of planetesimal diffusions.

We are currently investigating the three dimensional problem which appears to be far more difficult to analyze in the absence of any convenient coordinate system.

ACKNOWLEDGMENTS

It is a pleasure for A.N. to thank the Welsh Institute for Mathematical and Computational Sciences (WIMCS) for their financial support in this research. We would also like to thank Professor F.-Y. Wang of WIMCS for helpful conversations concerning parts of this work. Finally, A.T. would like to thank the Centro di Ricerca Matematica Ennio De Giorgi in Pisa for their hospitality during a research visit in July 2006 where some of the ideas in this work were developed.

[1] Bhatia, N. P. and Szegö, G. P., *Dynamical Systems: Stability Theory and Applications*, Lecture Notes in Mathematics Vol. 35 (Springer-Verlag, Berlin, 1967).
[2] Bhatia, N. P. and Szegö, G. P., *Stability Theory of Dynamical Systems*, Die Grundlehren der mathematischen Wissenschaften, Band 161 (Springer-Verlag, New York, 1970).
[3] Blanchard, P. and Golin, S., "Diffusion processes with singular drift fields," Commun. Math. Phys. **109**, 421–435 (1987).
[4] Bohr, N., "Uber die Anwendung der Quantentheorie auf den Atombau. I. Die Grundpostulaten der Quantentheorie," Z. Phys. **13**, 117–165 (1923).
[5] Buchholz, H., *The Confluent Hypergeometric Function with Special Emphasis on its Applications*, Springer Tracts in Natural Philosophy Vol. 15 (Springer-Verlag, New York 1969).

[6] Durran, R. and Truman, A., *Stochastic Mechanics and Stochastic Processes (Swansea, 1986)*, Lecture Notes in Mathematics Vol. 1325 (Springer, Berlin, 1988), pp. 76–88.
[7] Durran, R. and Truman, A., *Stochastic Analysis, Path Integration and Dynamics (Warwick, 1987)*, Pitman Research Notes Mathematics Series Vol. 200 (Longman, Harlow, 1989), pp. 197–214.
[8] Exner, P. and Truman, A., *Stochastics and Quantum Mechanics (Swansea, 1990)* (World Scientific, River Edge, NJ, 1992), pp. 130–150.
[9] Filippov, A. F., *Differential Equations with Discontinuous Righthand Sides*, Mathematics and its Applications (Soviet Series) Vol. 18 (Kluwer Academic, Dordrecht, 1988).
[10] Freidlin, M. I. and Wentzell, A. D., *Random Perturbations of Dynamical Systems*, Grundlehren der Mathematischen Wissenschaften [Fundamental Principles of Mathematical Sciences] Vol. 260, 2nd ed. (Springer-Verlag, New York, 1998).
[11] Lena, C., Delande, D., and Gay, J. C., "Wave functions of atomic elliptic states," Europhys. Lett. **15**, 697–702 (1991).
[12] Nelson, E., "Derivation of the Schrödinger equation from Newtonian mechanics," Phys. Rev. **150**, 1079–1085 (1966).
[13] Nelson, E., *Dynamical Theories of Brownian Motion* (Princeton University Press, Princeton, NJ, 1967).
[14] Nelson, E., *Quantum Fluctuations*, Princeton Series in Physics (Princeton University Press, Princeton, NJ, 1985).
[15] Simon, B., "Semiclassical analysis of low lying eigenvalues. I. Nondegenerate minima: asymptotic expansions," Ann. Inst. Henri Poincare, Sect. A **38**, 295–308 (1983).
[16] Simon, B., "Semiclassical analysis of low lying eigenvalues, II. Tunneling," Ann. Math. **120**, 89–118 (1984).
[17] Simon, B., "Semiclassical analysis of low lying eigenvalues. III. Width of the ground state band in strongly coupled solids," Ann. Phys. (N.Y.) **158**, 415–420 (1984).
[18] Simon, B., "Semiclassical analysis of low lying eigenvalues. IV. The flea on the elephant," J. Funct. Anal. **63**, 123–136 (1985).
[19] Truman, A. and Williams, D., *Recent Developments in Quantum Mechanics (Poiana Braşov, 1989)*, Mathematical Physics Studies Vol. 12 (Kluwer Academic, Dordrecht, 1991).
[20] Veretennikov, A. Yu., "On strong solutions of stochastic Itô equations with jumps," Teor. Veroyatn. Ee Primen. **32**, 159–163 (1987).
[21] Wang, F.-Y., *Functional Inequalities, Markov Semigroups and Spectral Theory* (Science, Beijing, 2005).
[22] Willems, J. L., *Stability Theory of Dynamical Systems* (Nelson, London, 1970).